Aus dem Institut für Immunologie und Molekularbiologie

des Fachbereichs Veterinärmedizin

der Freien Universität Berlin

Structural and functional analysis of LTBP 4 as a factor of pathogenesis in the development of pulmonary emphysema

Inaugural – Dissertation

zur Erlangung des Grades eines

Doktors der Veterinärmedizin

an der Freien Universität Berlin

Vorgelegt von

Katharina Dinger

Tierärztin

aus Villingen – Schwenningen

Berlin 2016

Journal-Nr.: 3769

Gedruckt mit Genehmigung

des Fachbereichs Veterinärmedizin

der Freien Universität Berlin

Dekan:	Univ. Prof. Dr. Jürgen Zentek
Erster Gutachter:	Prof. Dr. Michael F. G. Schmidt
Zweiter Gutachter:	Prof. Dr. Anja Sterner-Kock, PhD
Dritter Gutachter	Prof. Dr. Achim Gruber, PhD

Describtoren (nach CAB-Thesaurus): mice, animal models, pulmonary emphysma, postnatal development, transforming growth factor beta (MeSH), proteins, myofibroblast (MeSH), histology, elastic tissue (MeSH)

Tag der Promotion: 21.04.2016

Für meine Mutter

Table of contents

4

List of tables and figures

Tables

Figures

11

Abbrevations

ABE	actual base excess
αSMA	alpha smooth muscle actin
APS	ammonium persulfate
aqua dest.	distilled water
AZ	Aktenzeichen
B2M	beta-2-microglobulin
BMP	bone morphogenetic protein
cDNA	complementary DNA
cSMAD	common-mediator Smad
CTGF/Ctgf	connective tissue growth factor
ctHb	total haemoglobin
Cy3	cyanine dye nr. 3
DAPI	4`6-diamidino-2-phenylindole
DPBS	Dulbecco´s phosphate-buffered saline
DMEM	Dulbecco´s modified eagle medium
DMSO	dimethyl sulfoxide
DNA	desoxy ribonucleic acid

E	embryonic day
ECM	extracellular matrix
EGF	epidermal growth factor
FBS	fetal bovine serum
FGF	fibroblast growth factor
GAPDH	glycerinaldehyd-3-phosphat-dehydrogenase
H&E	hematoxylin and eosin staining
HCl	hydrogen chloride
Hct	hematocrit
HEL 299	human embryonic lung fibroblasts
HOPE	hepes glutamic acid buffer mediated organic solvent protection effect
HPRT	hypoxanthine-guanine phosphoribosyltransferase
IF	immunofluorescence
IgG	immunoglobulin G
IHC	immunohistochemical
JNK	C-Jun-N-terminal kinases

LANUV	Landesamt für Natur-, Umwelt- und Verbraucherschutz
LAP	latency associated protein
LLC	large latent complex
LTBP/Ltbp	latent TGFβ binding protein
M	molare Masse
MAPK	mitogen activated protein kinase
MEM	minimum essential media
MLECs	mink lung epithelial cells
mRNA	messenger RNA
NEAA	non essential amino acids
NRW	North Rhine-Westphalia
P	postnatal day
PAI-1/Pai-1	plasminogen activator inhibitor-1
Pen/Strep	penicillin streptomycin
PBS	phosphate-buffered saline
PCNA	proliferating cell nuclear antigen
PCR	polymerase chain reaction

PDGF-A	platelet-derived growth factor A
PFA	paraformaldehyde
pCO_2	partial pressure of carbon dioxide
pH	potential hydrogen
PI3K	phosphoinositide 3-kinase
pmol	picomol
pO_2	partial pressure of oxygen
RNA	ribonucleic acid
R-Smad	receptor-regulated Smads
RT-PCR	reverse transcriptase PCR
SDS	sodium dodecyl sulfate
SEM	standard error of the mean
siRNA	small interfering RNA
SLC	small latent complex
sO_2	oxygen saturation
p value	propability
PCR	polymerase chain reaction
TBS	tris buffered saline

TGFβ/ Tgfβ	transforming growth factor beta
VEGF	vascular endothelial growth factor
WB	western blot

1. Introduction

1.1. Lung organogenesis

Organogenesis of the mammalian lung includes a multitude of processes initiating with the primordium of the organ up to the branching of the airways and the maturation of the alveoli. There are two major goals of lung development: first to maximize the gas exchange surface area and second to minimize the blood air barrier (Roth-Kleiner and Post 2003, Copland and Post 2004). The complex architecture of the lung tissue is necessary to ensure an optimal oxygen supply and thereby the functionality and the viability of the organism. Lung development occurs in six distinct stages: (1) embryonic, (2) pseudoglandular, (3) canalicular, (4) saccular, (5) alveolar, and finally the (6) vascular maturation stage (Warburton, El-Hashash et al. 2010) (figure 1.1).
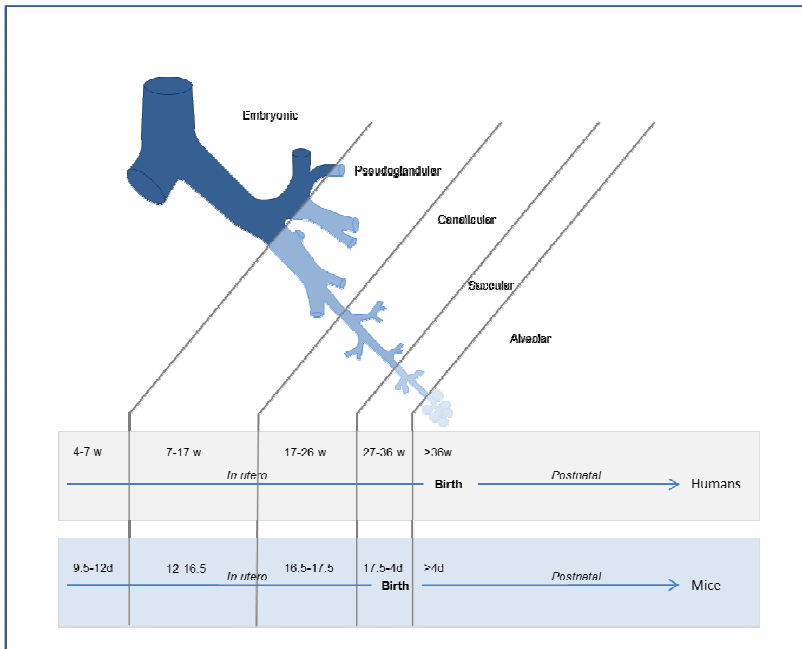
Figure 1.1 Schematic overview of lung development

Overview illustrating the morphological changes during the first five stages of lung development in humans and mice; stadium of vascularisation is not shown (modified after (Kajekar 2007), copyright (2016), with permission from Elsevier). Abbreviations used: w week, d day

These stages describe defined morphological changes and occur in a well balanced temporal pattern.

18

Two phases classify these sequential processes: the early phase, consisting of the first three stages, and the late phase, consisting of the last three stages of lung development, where the differentiation and maturation of the preformed lung tissue takes place (Warburton, El-Hashash et al. 2010).

1.1.1. Early lung development

Beginning with the outpouching of the lung buds from the anterior foregut in the embryonic stage (4-7 weeks after conception in humans, embryonic days 9.5-12 in mice) the early lung development passes through two further stages, the pseudoglandular (5-17 weeks after conception in humans, embryonic days 12-16.5 in mice) and the canalicular stage (16-26 weeks after conception in humans, embryonic days 16.5-17.5 in mice). Thereby the pseudoglandular stage is characterised by the branching of epithelial tubes lined with cuboidal epithelial cells. This fluid-filled primitive respiratory tree is then expanded in the canalicular stage, accompanied by angiogenesis and vascularisation, to achieve the

formation and subdivision of the airways as a framework for the respiratory tissue (Warburton, El-Hashash et al. 2010).

1.1.2. Late lung development

Late lung development is characterised by the process of alveolarisation, implying the formation and the increase of the respiratory tissue. During the saccular stage (24-38 weeks after conception in humans, embryonic day 17.5 until postnatal day 4 in mice) the distal airways form saccular dilatations, accompanied by a substantial thinning of the interstitium. These saccules comprise a double parallel network of capillaries, which can support air exchange in prematurely born human neonates and in murine neonates (Bourbon, Boucherat et al. 2005). At the end of alveolarisation the number of alveoli has increased sixfold. This process implicates a decrease of the alveolar air space and an increase of the total number of alveoli (Bourbon, Boucherat et al. 2005). Whilst the alveolarisation of the human lung starts in utero and persists until the postnatal period (36 weeks after

conception in humans – 36 months postnatal), the murine lung alveolarisation occurs entirely postnatal (postnatal days 4-28 in mice) (Schittny, Mund et al. 2008). During and after alveolarisation the premature double capillary networks are restructured to a mature single network in the stage of vascular maturation (Burri 2006, Warburton, El-Hashash et al. 2010).

1.2. Key factors of lung development

The afore mentioned morphological changes during lung development implicate highly coordinated cellular remodelling, cell migration, differentiation as well as extra cellular matrix (ECM) synthesis and assembly. The major focus of the early stages of lung development is on cell proliferation and apoptosis, while the late stages of lung development are characterised by cell migration and differentiation of highly specialised cell types to create a functional organ in utero, which is primed to the transition to air breathing and growth after birth (Warburton, El-Hashash et al. 2010). Two key factors

play an indispensable role for a finely concerted lung development. First cell differentiation and ECM deposition and second the biochemical regulation of lung development (Warburton, Schwarz et al. 2000, Jankov and Keith Tanswell 2004).

1.2.1 Cell differentiation and ECM deposition during lung development

Tissue formation during organogenesis requires the concerted action of numerous specialised cells. There are over 40 different highly specialised cell types emerging during lung organogenesis (Sorokin 1970, Rock and Hogan 2011), fulfilling a multitude of structural and functional duties. Beside the variety of somatic cells, like muscle cells, chondrocytes or vascular cells, there are several lung tissue specific cells, such as clara cells or alveolar epithelial type I and type II cells (Sorokin 1970). Focusing on the stage of postnatal alveolarisation, one cell type plays a pivotal role for a proper formation of

secondary septae in transition to air breathing, the myofibroblast (Bourbon, Boucherat et al. 2005).

1.2.1.1. Myofibroblasts

Myofibroblasts are distinctive fibroblasts found in different tissues, featured with a contractile apparatus that contains actin microfilaments with associated contractile proteins. The actin microfilaments align to bundles forming a specialised adhesion complex on the cell surface, the fibronexus (Singer, Kawka et al. 1984, Tomasek, Gabbiani et al. 2002). This complex enables the cell to link intracellular actin with extracellular matrix molecules like fibronectin. Functionally this enables the myofibroblasts to force generation and transmission of this load to the surrounding tissue (Brown, Prajapati et al. 1998).

	Fibroblast	Proto-Myofibroblast	Differentiated Myofibroblast
Characteristics	Cytoplasmatic β- /γ- actin	Cytoplasmic actin containing stress fibers	A-smooth muscle actin Super mature focal adhesions
Tissue	Normal connective tissue	Alveolar septum Early granulation tissue	Liver capsule Bone marrow stroma Late contracting granulation tissue Fibrocontractive disease
In vitro **model**	Low stiffness substrates ± TGF-β	Medium stiffness substrates	Medium stiffness substrates +TGF-β High stiffness substrates ± TGF-β Attached collagen gels

Figure 1.2 Characteristics of fibroblast-myofibroblast transdifferentiation

Drafts illustrate the morphological changes of fibroblasts during transdifferentiation, with the arrows indicating the required stimuli. The chart is specifying the characteristics of the cells in the different stages, the tissue localisation of the different cell types *in vivo* and the established *in vitro* model. Figure modified after (Tomasek, Gabbiani et al. 2002) copyright (2015), with permission from Elsevier.

Depended on the mechanical tension of the tissue, myofibroblasts appear in two different forms, non α-smooth muscle actin (αSMA) expressing proto-myofibroblasts in connective tissue under low tension and αSMA expressing, differentiated myofibroblasts in

24

connective tissue under high tension (figure 1.2) (Skalli, Ropraz et al. 1986, Dugina, Fontao et al. 2001, Hinz, Celetta et al. 2001).

1.2.1.2. Myofibroblast transdifferentiation

The process of transdifferentiation of fibroblasts into proto-myofibroblasts and differentiated myofibroblasts is elaborately described during skin wound healing (Tomasek, Gabbiani et al. 2002). Contraction of granulation tissue is a basic part during skin wound healing. After skin lesion fibroblasts migrate on a compliant substratum and the first wound closure is performed through tractional forces and reorganisation of the collagen matrix (Martin 1997, Heng 2011). With this initial closure of the wound the collagen fibres and fibroblasts orientate parallel to the wound along the expected lines of stress. As the resistance of the surrounding tissue increases during wound closure, transdifferentiation of fibroblasts into proto-myofibroblasts (in early granulation tissue) and differentiation into αSMA expressing differentiated

myofibroblasts (in late contracting granulation tissue) takes place (Tomasek, Gabbiani et al. 2002). In lung tissue both forms: proto-myofibroblasts and differentiated αSMA positive myofibroblasts are described (Kapanci, Ribaux et al. 1992). While proto-myofibroblasts appear as a constructive component of the alveolar septae, differentiated αSMA positive myofibroblasts localized at the alveolar entry ring seem to fulfil mechanical duties (Lindahl, Karlsson et al. 1997, McGowan, Grossmann et al. 2008).

1.2.1.3. Myofibroblasts in alveolarisation

During postnatal alveolarisation secondary septation of terminal air spaces is a key feature of the increase of the respiratory tissue (Warburton, El-Hashash et al. 2010). Myofibroblasts at the tips of the developing septae actively secret elastin. Elastin containing ridges spread from the saccule wall to become an alveolar septum with bundles of elastic fibres located at its apex (Lindahl, Karlsson et al. 1997, Bostrom, Gritli-Linde et al. 2002, Schittny, Mund et al. 2008). This elastin desposition and

subsequent elastic fibre formation is essential for the secondary septation of alveoli and normal alveolar development (figure 1.3).
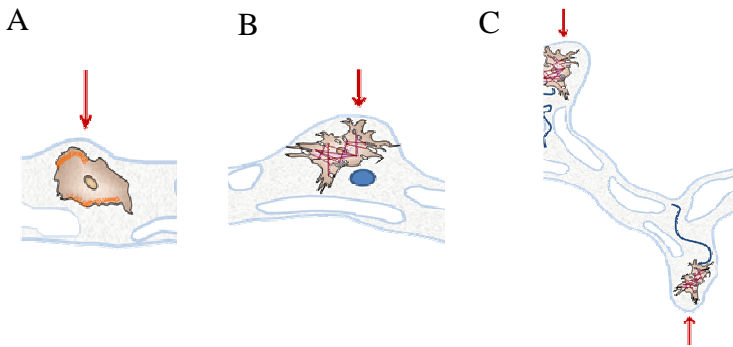
Figure 1.3 Diagram illustrating alveolarisation by secondary septation

Secondary septation initiates out of the preformed saccules (A). Ridges spread out of the primary septae, containing fibroblasts, which transdifferentiate and deposit elastin (B). At the end of septation, septae consist of in connective tissue embedded elastic fibres, with transdifferentiated myofibroblasts at the apexes. Red arrows indicate localization of newly formed secondary septae. Figure modified after (Schittny, Mund et al. 2008). Copyright (2015), with permission from Elsevier.

The detailed mechanisms of fibroblast transdifferentiation during late lung development are just beginning to be understood. However, *in vitro* studies on murine fibroblasts isolated from various connective tissues and cultured under different conditions gave first insights into myofibroblast transdifferentiation and its dependency on cellular-matrix interaction (Tomasek, Gabbiani et al. 2002). Fibroblasts grown in three dimensional hydrated collagen lattices differentiate dependent on the substrate stiffness (Figure 1.2). In free floating untethered collagen lattices with low stiffness fibroblasts maintain their phenotypic proportions. Mimicking the incidents during wound closure, fibroblasts placed into these collagen lattices align the collagen matrix and develop tractional forces. Due to these mechanisms the diameter of free floating lattices is reduced over time (Grinnell 2000). By increasing the stiffness of the substrate to a medium level, tension develops and fibroblasts acquire the proto-myofibroblast phenotype and form stress fibres, adhesion complexes

and fibronectin fibrils. Maintenance of the proto-myofibroblast phenotype requires a constant resistance of the matrix to cellular tractional forces. Disintegration of this matrix – cell interaction, by inhibiting the actin-myosin force generation or by lowering the stiffness of the substrate, results in a loss of the proto-myofibroblast phenotype. Growing fibroblasts in high stiffness substrates or attached collagen gels sustaining a high resistance of the substrate over a longer period of time, results in a transformation of proto-myofibroblasts into differentiated αSMA expressing myofibroblasts (Tomasek, Haaksma et al. 1992).

1.3. Biochemical regulation of lung development

Both early and late lung development are sequences of finely-tuned processes, which are tightly regulated by the concerted action of growth factors, transcription factors, and mechanical stretching (Warburton, Schwarz et al. 2000, Roth-Kleiner and Post 2003, Jankov and Keith

Tanswell 2004, Warburton, El-Hashash et al. 2010).There are several growth factors mentioned during lung development, notable amongst them are bone morphogenetic protein (BMP), epidermal growth factor (EGF), fibroblast growth factor (FGF) and transforming growth factor β (TGFβ). While BMP, EGF and FGF play a pivotal role during early lung branching morphogenesis (Min, Danilenko et al. 1998, Hokuto, Perl et al. 2003) TGFβs play a key role during the whole lung development, regulating proliferation, transformation, ECM deposition and apoptosis (Roth-Kleiner and Post 2003, Jankov and Keith Tanswell 2004). In addition TGFβ1 plays a crucial role in myofibroblast trandifferentiation (Tomasek, Gabbiani et al. 2002).

1.3.1. TGFβ in mammalian lung tissue

TGFβ with its isoforms belongs to a superfamily of different cytokines such as activin or BMP. Five isoforms of TGFβ have been described so far: TGFβ5 in Xenopus laevis (Kondaiah, Taira et al. 2000), TGFβ4in chicken (Pan and Halper 2003) and three tissue specific forms of

TGFβ (TGFβ1-3) in mammals (Beyer, Narimatsu et al. 2012). Whereas TGFβ1 is globally expressed in lung mesenchyme, particularly underlining distal epithelial branching points, TGFβ2 is predominantly localized in distal epithelium and TGFβ3 in proximal mesenchyme and mesothelium (Pelton and Moses 1990, Millan, Denhez et al. 1991, Pelton, Johnson et al. 1991, Schmid, Cox et al. 1991, Bragg, Moses et al. 2001). Isoform specific knockouts have revealed a non-redundant role of each of the three TGFβ isoforms.

While Tgfβ1$^{-/-}$ mutation in mice leads to lethal pulmonary inflammation within two months of life (McLennan, Poussart et al. 2000), Tgfβ2$^{-/-}$ mutation results in embryonic lethality associated with cardiac anomalies and lung dysplasia (Bartram, Molin et al. 2001). Deficiency of Tgfβ3 in mice causes retarded lung development and neonatal lethality (Kaartinen, Voncken et al. 1995, Shi, Heisterkamp et al. 1999).

1.3.2. TGFβ signalling

TGFβ signalling is mediated in a cascade like fashion, introduced by binding of active TGFβ to the transmembrane TGFβ receptor II, which leads to the assembly with transmembrane TGFβ receptor I. This receptor complex transmits signals by means of phosphorylation and therefore activation of second messenger molecules such as Smad proteins or Smad independent pathways like mitogen activated protein kinase (MAPK), phosphoinositide 3kinase (PI3K) and C-Jun-N-terminal kinases (JNK) pathways. Smads are a family of cytoplasmic signal transducer proteins consistent of three classes of Smad; first the receptor-regulated Smads (R-Smad) including Smad1, Smad2, Smad3, Smad5, and Smad8/9, second the common-mediator Smad (co-Smad) namely Smad4 and third inhibitory Smads (I-Smads) including Smad 6 and Smad 7 (Chen, Hata et al. 1998, Massague 1998). During TGFβ signal transduction, activated R-Smads such as Smad2 and Smad3 bind to co-Smad4. This complex translocates

to the nucleus and activates the transcription of matrix components including fibronectin, type I collagen, laminin, and glycosaminoglycans. TGFβ acts as a potent stimulatory signal for connective tissue formation, mediated via indirect mechanisms involving amongst others connective tissue growth factor (CTGF) and plasminogen activator inhibitor-1 (PAI-1) (Grotendorst, Martin et al. 1985, Iwaki, Urano et al. 2012). Transgenic mouse technology has revealed that both proteins play a pivotal role in the regulation of ECM composition and their deregulation is connected to lung fibrotic diseases. Overexpression of Ctgf decreases alveolarisation and vascular development in a mouse model (Chen, Rong et al. 2011). Deletion of the *Pai-1* gene reduces the susceptibility to lung fibrosis induced by different stimuli and overexpression of Pai-1 enhances the susceptibility of mice to lung fibrosis (Eitzman, McCoy et al. 1996)

1.3.3. TGFβ signalling in lung development

Both timing and dosage of TGFβ signalling are critical during early and late lung development (Alejandre-

Alcazar, Michiels-Corsten et al. 2008). It was shown, that overexpression as well as inhibition of TGFβ impacts alveolarisation. Rodents over-expressing Tgfβ1 due to adenoviral transfer of Tgfβ1 (Gauldie, Galt et al. 2003) or by conditional overexpression of bioactive Tgfβ1 (Vicencio, Lee et al. 2004) displayed defective alveolarisation. In contrast, blockade of Tgfβ signalling in Smad3 deficient mice (Chen, Sun et al. 2005) resulted in progressive airspace enlargement and disruption of alveolarisation. In addition TGFβ1 signalling is dynamically regulated over the course of late lung development (Alejandre-Alcazar, Michiels-Corsten et al. 2008). *In vivo* studies suggest, that endothelial maturation is stimulated, while production of ECM is gradually downregulated by dynamic regulation of TGFβ1 signalling during late lung development (Alejandre-Alcazar, Michiels-Corsten et al. 2008).

1.4. Latent TGFβ Binding Protein (LTBP)

1.4.1. Regulation of the bioavailability of TGFβ through LTBPs

Cells secrete TGFβ in a biological inactive form, non-covalently bound to its propeptide. Hence the propeptide renders TGFβ inactive; it is named latency associated protein (LAP) whereas the complex between TGFβ and LAP is named the small latent complex (SLC). Although this latent complex is secreted into the ECM, the release of the large latent complex (LLC) is even more effective (Oklu and Hesketh 2000). At this compound the latent TGFβ Binding Protein (LTBP) binds the SLC and binds it to the ECM (figure 1.4). Therefore the ECM acts as a TGFβ reservoir and enables a fast release of TGFβ without new synthesis. To activate TGFβ from its inactive in its biologically active form; cleavage of LTBP is necessary, which can be performed by different factors, such as proteases, integrins, thrombospondin,

reactive oxygen species and low or high pH (Chandramouli, Simundza et al. 2011).
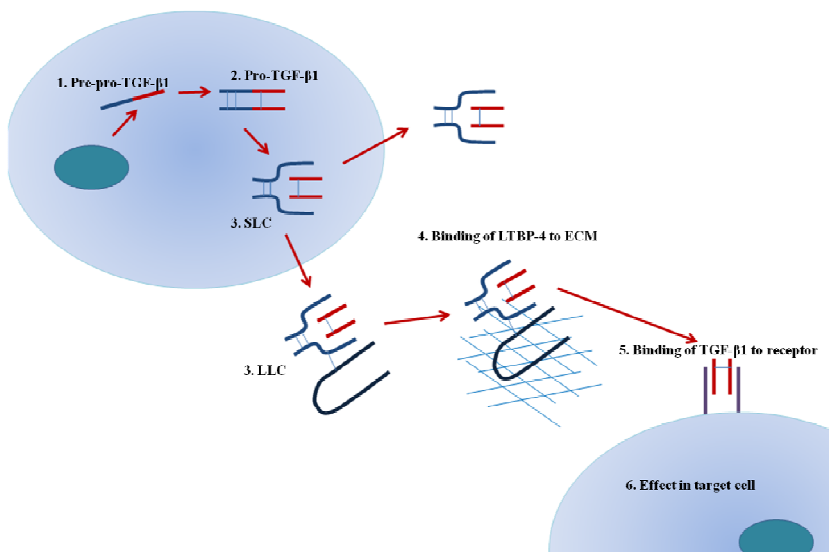
Figure 1.4 Schematic illustration of the regulation of the bioavailability of TGFβ through LTBPs

TGFβ is secreted out of the nucleus, bound to its propeptid, the LAP, forming the SLC. The SLC is either secreted directly into the ECM or bound to LTBP forming the LLC. This LLC stabilizes TGFβ and maintains it at the ECM. Cleavage of TGFβ allows binding to the receptor, and subsequent signalling.

1.4.2. Structure of LTBPs

LTBPs are large extracellular microfibrillar glycoproteins and structurally related to fibrillins (Todorovic and Rifkin 2012). Sixty percent of the LTBP protein are composed of Epidermal-Growth-Factor like domains (EGF-like domains) and four cystein rich domains (Sterner-Kock, Thorey et al. 2002) (Figure 1.5).

4-Cystein domain

Non Ca^{++}binding EGF-like domain

8-Cystein domain

Ca^{++}binding EGF-like domain
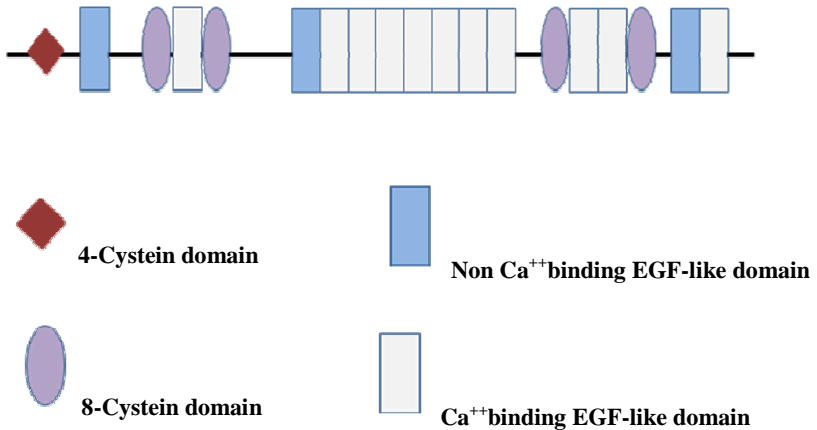
Figure 1.5 Schematic diagram of the protein domain structure of LTBP4

Figure modified from (Saharinen, Hyytiainen et al. 1999) copyright (2015), with permission from Elsevier.

The cystein rich domains are a distinctive feature, which can only be found in fibrillin and LTBPs. The third cystein rich domain forms the binding site of TGFβ bound to its propeptide (Todorovic, Jurukovski et al. 2005). The N- and C- terminus link the protein to the ECM, while the N- terminus interacts with fibronectin, the C-terminus can interact with fibrillin, respectively. Today four isoforms of LTBPs (LTBP1-4) are known in mammals. LTBP1, -3 and -4 can bind latent TGFβ1, whereas LTBP2 does not (Oklu and Hesketh 2000). All four isoforms are expressed in a tissue specific manner (Oklu and Hesketh 2000) (table 1.6).

Isoforms	LTBP1	LTBP2	LTBP3	LTBP4
Expression pattern	Heart	Lung	Heart	Heart
	Lung	Muscle	Muscle	Muscle
	Placenta	Liver	Ovaria	Liver
		Placenta	Placenta	Lung
Human splicevariants	LTBP1l	-	-	LTBP4l1
	LTBP1s			LTBP4l2
				LTBP4s
Murine splicevariants	Ltbp1l	-	-	Ltbp4l
	Ltbp1s			Ltbp4s

Table 1.6 Diagram illustrating distribution of different LTBP isoforms

The chart lists the four different isofoms, their expression pattern in the tissue and their human and murine splicevariants (Oklu and Hesketh 2000). Copyright (2015), with permission from Elsevier.

Mice with null mutations of the genes for the different isoforms display distinct phenotypic abnormalities:

Ltbp1l^{-/-} mutation in mice leads to a disruption in the development of heart, lung and bones (Yoshinaga, Obata et al. 2008).

Ltbp2^{-/-} mutation in mice leads to embryonic lethality (Shipley, Mecham et al. 2000).

Ltbp3^{-/-} mutation in mice leads to retarded lung development and abnormal bone morphology (Colarossi, Chen et al. 2005).

Alternative splicing results in structural variability. Two independent promotors are described for LTBP1 and LTBP4, resulting in two major splice variants, a long form (LTBP1l, LTBP4l) and a short form (LTBP1s; LTBP4s), respectively (Koski, Saharinen et al. 1999). Ltbp4s mutation in mice leads to developmental abnormalities in lung, cardiomyopathy and colorectal cancer (Sterner-Kock, Thorey et al. 2002). However a

detailed expression pattern of the different splice variants has not been reported so far.

It has been shown, that the long form of LTBP4 binds TGFβ much more efficiently than the short isoform (Kantola, Ryynanen et al. 2010). LTBP2 and LTBP4 are believed to be components of the microfibrils that surround the elastin core of elastic fibres (Saharinen, Hyytiainen et al. 1999).

Taken together, these observations suggest that LTBP4 executes at least two functions: on the one hand as a regulator of secretion, latency, storage and activation of TGFβ in the ECM and on the other hand as a distinct structural protein of the ECM (Dabovic, Chen et al. 2009).

1.5. Diseases associated with LTBP4

Ltbp4s knockout mice (3C7)

Homozygous mice, lacking the short isoform of Ltbp4 (3C7-mice) develop severe lung emphysema and

cardiomyopathy (Sterner-Kock, Thorey et al. 2002). Immunohistochemical staining of tissue sections had shown a significant decrease of the extracellular Tgfβ1 level in lung, heart and colon of the homozygous animals. Histologically, these animals had incomplete septal walls of alveoli. Tissues of lung, colon and heart showed incomplete, fragmented elastic fibre formation with multiple patches of condensed elastin. This resulted in an almost complete loss of pulmonary elasticity. Secondary changes in the protein structure of the matrix were also detectable (Sterner-Kock, Thorey et al. 2002).

Ltbp4$^{-/-}$ mice (E301B04)

Ltbp4$^{-/-}$ mice (E301B04) were generated recently in our lab, using a commercially available embryonal stem cell. Genotyping of litters revealed a genotype division after mendelian ratio (Bultmann-Mellin et al. 2015).

Quantitative RT-PCR analysis and western blot analysis of tissue of Ltbp4$^{-/-}$ mice confirmed a complete loss of

Ltbp4. Ltbp4$^{-/-}$ mice die within the first ten days of life, after acute respiratory distress.

Clinical manifestations in humans caused by mutations of the *LTBP4* gene are rare. To date there are only four published cases of children suffering from Urban Rifkin Davis syndrome (URDS) caused by mutations of the *LTBP4* gene (Urban, Hucthagowder et al. 2009) and one publication discussing mutational analyses on cutis laxa patients (Callewaert, Su et al. 2013).

Urban Rifkin Davis syndrome (URDS)

In 2009 Urban et al. reported in the American Journal of Human Genetics four cases of newborn children with impaired pulmonary, gastrointestinal, genitourinary, musculoskeletal, and dermal development (Urban, Hucthagowder et al. 2009). Despite a huge variety of the disease pattern, clinical findings can be concluded to developmental defects and structural changes of the connective tissue. Respiratory lesions implied severe bronchopulmonary dysplasia, lung emphysema and

atelectatic abnormalities. Mutational analysis revealed that all four patients had autosomal recessive mutations in the *LTBP4* gene (Figure 1.7).
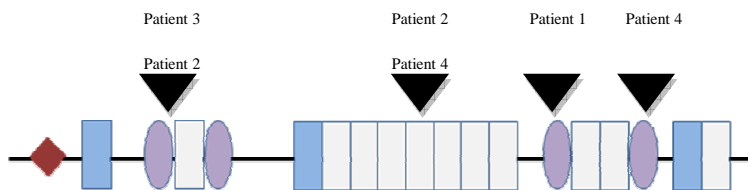
Patient	Exon	Domain	Status	Gene	cDNA	Protein
1	28	8-CYS$_2$	hom	g.29481delA	c.3554delA	p.Q1185fsX1211
2	9	HYB	het	g.12574	c.791delC	P264fsX300
	22	EG$_{11}$	het	g.25287_25288delGCinsAA	c.2570_2571delGCinsAA	p.C857X
3	9	HYB	hom	g.12603T>G	c.820T>G	p.C274G
4	22	EG$_{11}$	het	g.20287_20288delGCinsAA	c.2570_2571delGCinsAA	p.C857X
	33	8-CYS$_3$	het	g.33861insC c.4128insC		p.P1376fsX1403

Figure 1.7 Schematic representation of the domain structure of LTBP4, showing the location of the mutations found in URDS patients

Patient 1: Homozygous for mutation p.Q1185fsX1211 died with 9 month

Patient 2: Heterozygous for two different mutations (P264fsX300, p.C857X) died with 4 month

Patient 3 Homozygous for mutation p.C274G survived

Patient 4: Heterozygous for two mutations (p.C857X, p.P1376fsX1403), died with 23 month

Abbrevations are as follows: EG, EGF-like domain; HYB, hybrid domain; 8-CYS, 8cysteine domain; het, heterozygous; hom, homozygous. Figure modified from Urban et al. 2009 copyright (2015), with permission from Elsevier.

Three patients died of respiratory failure in infancy or early childhood (Urban, Hucthagowder et al. 2009). Autopsy and histological analyses of tissue sections of one patient (patient 2) showed an impaired elastic fibre and tissue architecture in the lung. (Figure 1.8).
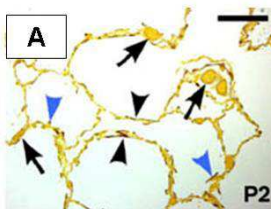
Figure 1.8 Tissue section of URDS patient 2

Lung section of patient 2 with enlarged saccular airspace and fragmented elastic fibre s confined to the saccular wall (blue arrowheads) and to arrested septae (black arrowheads). Cappillaries are enlarged and have thickened walls (black arrows) (Urban, Hucthagowder et al. 2009).

The molecular defects were associated with blocked alveolarisation (Urban, Hucthagowder et al. 2009). One patient (patient 3) survived. Physical exams at seven years of age were significant for cutis laxa. The patient fatigues early, uses a speaking valve, can say about 80 words and has difficulties in jumping or running. In contrast to the other patients mutational analysis had shown a single base deletion in the first cystein domain of LTBP4.

Based on the fact that URDS patients exhibit cutis laxa, mutational analyses on cutis laxa patients were performed, investigating a correlation between LTBP4 disruption and cutis laxa. Interestingly, all cutis laxa patients, positive for a mutation in the *LTBP4* gene,

present with pulmonary emphysema (Callewaert, Su et al. 2012).

1.6. Outline of the thesis

LTBP4 deficient individuals, humans and mice, die in the stage of postnatal alveolarisation after acute respiratory distress (Sterner-Kock, Thorey et al. 2002, Urban, Hucthagowder et al. 2009).

LTBP4 is known to execute at least two functions: as a regulator of the bioavailability of TGFβ1 and as a distinct structural protein of the ECM (Dabovic, Chen et al. 2009).

With regard to preceding studies a proper structured ECM combined with a dynamic regulation of TGFβ 1 is inalienable for myofibroblast transdifferentiation. However to date there are no publications linking myofibroblast transdifferentiation to LTBP4. Therefore we aimed this study to test the following hypothesis:

"Deficiency of LTBP4 leads to disrupted postnatal alveolarisation, resulting in lung emphysema, due to aberrant myofibroblast transdifferentiation."

The proposed project has three specific sub aims:

To analyse phenotypic changes of the lung tissue of Ltbp4$^{-/-}$ mice

To decipher dysregulated key processes of postnatal lung development in Ltbp4$^{-/-}$ mice

To functionally characterise underlying molecular mechanisms of myofibroblast transdifferentiation in Ltbp4$^{-/-}$ mice

By investigating the impact of LTBP4 on the myofibroblast transdifferentiation during late lung development, we pursue the overall goal to get a broader understanding of the functions of LTBP4.

2. Materials and Methods

2.1. Materials

2.1.1. Standard solutions

Solutions for cell culture experiments

Tissue lysis buffer

170 U/ml Collagenase Type I

2.4 U/ml Dispase in DPBS

1.76x MEM

8.8 ml MEM 10x

5000 units Pen/Strep

1.8 mM Na_2CO_3 in H_2O

Add 50 ml (aqua dest.) (sterile filtration)

Solutions for histology

Citrate buffer

Solution A: 100 mM Citrat acid

Solution B: 100   mM   Trinatriumcitrat   Dihydrat
$C6H5Na_3O_7$ x $2H_2O$

18ml Solution A + 82ml Solution B ad 1 l *aqua dest.* pH
6.0

Hart´s stain

1 volume Weigert´s resorcin fuchsin (Waldeck, Münster,
Germany)

9 volumes 1% Hydrochloric acid in 70% ethanol

Weigert´s hematoxylin

1 volume Weigert´s iron hematoxylin A (Waldeck,
Münster, Germany)

1 volume Weigert´s iron hematoxylin B (Waldeck,
Münster, Germany)

Solutions for western blot analyses

Lower gel buffer

1.5 M Tris/HCl pH 8.8

0.4 % (w/v) SDS

Upper gel buffer

0.5 M Tris/HCl pH 6.8

0.4 % (w/v) SDS

Blotting buffer (10x)

1.92 M Glycin

0.25 M Tris

Electrophoresis buffer (10x)

1.92 M Glycin

0.25 M Tris

1 % (w/v) SDS

TBST (10x)

1.5 M NaCl

100 mM Tris/HCl, pH7.5

Before usage add 0.05 % (v/v) Tween 20 to 1x TBS

ECL Solution

Solution A: 0.1 M Tris/HCl (pH 8.6)

0.02 mM/ml Luminol

Solution B: 0.0068   mM/ml   para-Hydroxycoumarin acid in DMSO

2.1.3. Antibodies

Primary antibodies for Western blot analyses, immunocytochemistry and histology are listed below

Antibody	Name	Reactivity	Origin	Dilution / Application	Company
Alpha smooth muscle actin	C6198-clone 1A4	murine	Purified mouse immunoglobulin	1:200 IF 1:200 WB	Sigma-Aldrich
GAPDH	14C10	human, murine	Purified rabbit immunoglobulin	1:1000 WB	Cell Signalling
LTBP4	GTX101725	human	Purified rabbit immunoglobulin	1:200 WB	GeneTex
Ltbp4	AF2884	murine	Purified goat immunoglobulin	1:100 IHC 1:1000 WB	R&D Systems
PCNA	E285RUO	human, murine	Purified rabbit immunoglobulin	1:200 IHC	Spring Bioscience
Vimentin	D21H3	human, murine	Purified rabbit immunoglobulin	1:600 IF	Cell Signalling

Table 2.1 List of primary antibodies

Secondary antibodies

For immunohistochemical studies, staining was revealed using DCS Supervision detection kit (DCS, Hamburg, Germany).

For immunofluorescence staining, goat anti-rabbit IgG Alexa-488 (Life Technologies, Darmstadt, Germany) was used as secondary antibody.

2.1.4. Primers for qRT-PCR

All primers were purchased from Eurofins MWG operon (Ebersberg, Germany).

Name	Species	FASTA sequence	Sequence	Product size
hB2M for	human	NM004048.2	CTCCGTGGCCTTAGCTGTG	69 bp
hB2M rev	human		TTTGGAGTACGCTGGATAGCCT	
mB2m for	murine	NM009735.3	CACTGACCGGCCTGTATGCT	64 bp
mB2m rev	murine		GGTGGGTGGCGTGAGTATACTT	
hCTGF for	human	NM001901	TTGGCCCAGACCCAACTATG	121 bp
hCTGF rev	human		CAGGAGGCGTTGTCATTGGT	

Name	Species	FASTA sequence	Sequence	Product size
mCTGF for	murine	NM010217.2	AGCTGACCTGGAGGAAAACA	70 bp
mCTGF rev	murine		GACAGGCTTGGCGATTTTAG	
hGAPDH for	human	NM002046.4	GCCATCAATGACCCCTTCATT	89 bp
hGAPDH rev	human		TTGACGGTGCCATGGAATTT	
mGapdh for	murine	NM008084.2	ATGTGTCCGTCGTGGATCTGA	80 bp
mGapdh rev	murine		TGCCTGCTTCACCACCTTCT	
hHPRT1 for	human	NM000194.2	TGACACTGGCAAAACAATGCA	94 bp
hHPRT1 rev	human		GGTCCTTTTCACCAGCAAGCT	
mHprt 1 for	murine	NM013556.2	CTGGTGAAAAGGACCTCTCG	91 bp
mHprt 1 rev	murine		CAAGGGCATATCCAACAACA	
hLTBP4 for	human	NM001042544.1	GCT GCC CTG TGT GAA AAT GTC	119 bp
hLTBP4 rev	human		GGG AAC GTG CCA GCA GAA	

Name	Species	FASTA sequence	Sequence	Product size
hPAI-1 for	human	NM000602.4	GAGGTGCCTCTCTCTGCCCTCACCAACATT	183 bp
hPAI-1 rev	human		AGCCTGAAACTGTCTGAACATGTCG	
mPai-1 for	murine	NM008871.2	CCCCACGGAGATGGTTATAG	87 bp
mPai-1 rev	murine		ATCACTTGGCCCATGAAGAG	

Table 2.2 List of qPCR primers

2.1.5. siRNA

siRNA was applied as a mixture of four different LTBP4 specific siRNA (On-Target Plus siRNA SMART pool) and purchased from Dharmacon (item number: L-019552-00-0005 Dharmacon, Lafayette, CO, USA).

2.1.6. Software

Axiovision Zeiss Imaging Software, Carl Zeiss AG (Jena, Germany)

BioDoc Analyse 2.1 (Göttingen, Germany)

Cell D 3.4 Olympus Soft Imaging Solutions GmbH (Hamburg, Germany)

geNorm version 3.5, PrimerDesign Ltd. (Southampton, UK)

GraphPad Prism Software 1.0 (San Diego, Ca, USA)

Image Lab 4.0.1., BioRad (Munich, Germany)

2.2. Methods

2.2.1. Animal work

All animal procedures were approved by the government of the State of North Rhine-Westphalia (AZ 8.84-02.05.20.11.097 LANUV, NRW). Ltbp4$^{-/-}$ mice of the second generation (F1) and wildtype littermates (C57BL/6N) were used in all studies.

2.2.1.1. Trunc blood analyses

At postnatal day eight pups were sacrificed by decapitation. Trunc blood was collected in a micro

haematocrit tube (Brandt, Wertheim, Germany) and analysed using ABL800 FLEX blood gas analyser (Radiometer, Willich, Germany). Samples were tested for pH, pCO_2, pO_2, ctHb, sO_2, Hct, $cHCO_3^-$, ABE.

2.2.1.2. Tissue processing

For further analyses pups were euthanized at postnatal day eight as follows. Following anesthesia with ketamine (100mg/kg body weight, Pfizer, Berlin, Germany) and xylazine (5mg/ kg body weight, Bayer, Leverkusen, Germany) the animals were exsanguinated by aortic transection. The right main bronchus was ligated and the right lung was resected and splitted. One part was snap frozen (for RNA and protein analyses) and the other part was stored in ice cold sterile DPBS for isolation of primary lung fibroblasts (see 2.2.2.2.) For histological and histomorphometric analyses the left lungs were inflated with 4% buffered PFA. Fixative was delivered through the cannulated trachea with an underwater pressure of 10 cm. After fixation tissue was processed

and embedded in paraffin. Three-micrometer sections were used in all studies.

2.2.1.3. Histology

All tissue sections were deparaffinised three times in xylene (Roth, Karlsruhe, Germany) for 10 minutes and rehydrated through a decreasing ethanol gradient (100% ethanol, 96% ethanol, 80% ethanol, 70% ethanol, *aqua dest.*; 1 minute each).

Hematoxylin and eosin staining of lung sections

For histomorphometric analysis, sections were stained with hematoxylin and eosin. After 3 minutes of incubation in Gill´s hematoxylin (VWR, Darmstadt, Germany) sections were washed in *aqua dest.*, differentiated for 10 minutes in tap water and transferred to eosin staining solution (Roth, Karlsruhe, Germany) for 6 minutes. Tissue sections were washed three times in *aqua dest.*, rehydrated through an increasing ethanol

gradient (70% ethanol, 80% ethanol, 96% ethanol, 100% ethanol, 1 minute each), incubated in xylene (Roth, Karlsruhe, Germany) and mounted with entelan (Merck,Darmstadt, Germany).

Histomorphometric analysis of lung sections

For histomorphometric analysis the mean linear intercept was measured by light microscopy using an Olympus BX 40 microscope (Olympus, Hamburg, Germany) on hematoxylin and eosin stained lung sections (see 2.2.1.3.). Six animals per genotype were analysed, ten sections per animals were stained, five random fields were photographed under 20 x magnifications, and 10 horizontal lines were drawn across each field. Large airways, vessels and atelectatic areas were avoided. Each intercept of the lines and alveolar walls was counted and the total number of intercepts per field was divided through the total length of lines. Pictures were acquired

and evaluated using Cell D 3.4 Olympus Soft Imaging Solutions (Olympus, Hamburg, Germany).

Ltbp4 staining of lung sections

To assess Ltbp4 expression in murine lung sections, tissue sections were boiled in citrate buffer pH 6 for 25 minutes and stained with antibody against Ltbp4 (see 2.1.3.). Signal detection was revealed using DCS Supervision detection kit (DCS, Hamburg, Germany). Slides were counterstained with hematoxylin. Pictures were taken at 10 x magnification using Olympus BX 40 (Olympus, Hamburg, Germany) and Cell D 3.4 Olympus Soft Imaging Solutions (Olympus, Hamburg, Germany).

Hart staining of lung sections

To survey the distribution and morphology of elastic fibres, lung tissue sections were stained with Hart´s staining solution.

Sections were brought into water via xylene and alcohol (see 2.2.1.3.) and afterwards incubated in Hart´s solution

(see 2.1.2.) overnight. The next day sections were washed with 95% ethanol, differentiated with 1 % acid alcohol and washed with tap water. After rinsing with *aqua dest*, sections were counterstained with Weigert´s hematoxylin (see 2.1.2.) for 10 minutes. Slices were washed with *aqua dest.*, differentiated with 1% acid alcohol for 5 seconds and tap water for 5 minutes. Counterstaining was revealed with van Gieson´s picro fuchsin (Waldeck, Münster, Germany) for 30 seconds.

After staining, slices were washed with 96% ethanol, dehydrated through an increasing ethanol gradient (70% ethanol, 80% ethanol, 96% ethanol, 100% ethanol) cleared with xylene (Roth, Karlsruhe, Germany) and mounted with entelan (Merck,Darmstadt, Germany).

Anti smooth muscle actin staining of lung sections

To mark myofibroblasts, lung tissue sections were stained with antibody against anti smooth muscle actin Cy3 labelled (see 2.1.3.). Counterstaining was revealed

with DAPI (Life Technologies, Karlsruhe, Germany). Sections were mounted aqueous using Dako Faramount mounting medium (Dako, Hamburg, Germany). Pictures were taken at 20 x magnification. Images were captured using Axiovert 200 and Axiovsion Imaging Software (Carl Zeiss, Jena, Germany).

2.2.2. Cell culture

All used media for cell culture contained 10 % FBS and 1 % Pen/Strep solution and were purchased from Life Technologies.

2.2.2.1. Human embryonic lung fibroblasts

Human embryonic lung fibroblasts (HEL299, ATCC Catalogue Number CCL-137) were a generous gift of Prof. Dr. med Racké (University of Bonn, Germany). Cells were cultured in MEM (Life Technologies, Darmstadt, Germany), supplemented with 1% NEAA (Life Technologies, Karlsruhe, Germany) at 5 % CO_2

concentration and 37°C under humid conditions. Cells were used at passage three after 24 hours of starvation in FBS free media.

Transfection of human embryonic lung fibroblasts

Human embryonic lung fibroblasts (HEL299) were transiently transfected with On-Target Plus siRNA pool specific for LTBP4 (Dharmacon, Lafayette, CO, USA). 24 hours prior transfection, cells were seeded in 6-well culture dishes (Sarstedt, Newton NC, USA) in a concentration of 80 000 cells per well. Cells were transfected with 100 pmol siRNA with 5 µl Lipofectamine2000 (Life Technologies, Darmstadt, Germany) following manufacturer´s protocol. As control served mock transfected cells, only treated with transfection reagent. 72 hours post transfection cells were trypsinized and seeded on 10 cm culture dishes (Sarstedt, Nümbrecht). 96 hours post transfection cells were retransfected with 200 pmol and 10 µl

Lipofectamine2000. 48 hours later cells were harvested for further experiments.

2.2.2.2. Isolation of primary murine lung fibroblasts

Primary murine lung fibroblasts were isolated at postnatal day eight (see 2.2.1.2.) using a one-step incubation procedure. Lung tissue was minced in DPBS and then digested for 180 minutes at 37°C degree on a shaker using tissue lysis buffer (see 2.1.2.). After digestion cells were sedimented and resuspended in DMEM, filtered through a 70 µm cell strainer (BD Bioscience, Heidelberg) and expanded in monolayer culture for three passages in DMEM at $5\% CO_2$ concentration and 37°C. Cell number and viability were determined with a haemocytometer using trypan blue staining. Culture purity was assessed at passage three via immunofluorescence through determination of cells expressing vimentin. Only pure cell cultures were used

for experiments. Cells were used at passage three after 24 hours of starvation in FBS free media.

Immunocytochemistry of primary murine lung fibroblasts

To analyse culture purity, isolated primary murine lung fibroblasts (see 2.2.2.2.) were grown on glass cover slips (VWR international, Darmstadt, Germany) in 24 well dishes overnight. Next day cells were fixed with -20°C cold methanol. Expression of vimentin was assessed using anti vimentin antibody (see 2.1.3.). Immune complexes were visualized with goat anti-rabbit IgG Alexa-488 (Life Technologies, Darmstadt, Germany) secondary antibody. Cell nuclei were counterstained with DAPI (Life Technologies, Darmstadt, Germany). Stained cells were washed and aqueous mounted (Dako, Faramount, Hamburg, Germany). Images were captured using Axiovert 200 and Axiovision Imaging Software (Carl Zeiss, Jena, Germany).

Stimulation of primary murine lung fibroblasts with TGFβ1

To test the influence of TGFβ1 on primary murine lung fibroblasts, cells were seeded in 3.5 cm cell culture dishes (Sarstedt, Nürmbrecht). After 12 hours of starvation, cells were incubated in DMEM supplemented with PBS, 1 ng or 2 ng human recombinant TGFβ1 (Biochrom AG, Berlin, Germany) at 5% CO_2 concentration and 37°C for 48 hours. Subsequently cells were harvested and qRT-PCR was performed (see 2.2.3.1).

2.2.2.3. Relaxed collagen lattices

To test the ability of cells to contract a deformable substrate, lung fibroblasts were grown in relaxed collagen lattices. Murine (see 2.2.2.2.) and human primary lung fibroblasts (see 2.2.2.1.) were harvested through trypsinization, counted with a haemocytometer using trypan blue staining. Cells were seeded on ice in a concentration of 200 000 cells per lattice into relaxed

collagen gel mix consisting of 0.92 ml 1.76 x MEM, 0,4 ml Collagen I, Rat tail (Life Technologies, Darmstadt, Germany), 0.1 ml 0.1 M NaOH and 0.2 ml FBS (Biochrom AG, Berlin, Germany). Suspension was added to 3.5 cm petri dishes (Sarstedt, Newton NC, USA). Lattices were incubated at 5 % CO_2 concentration and 37 °C. Rates of gel contraction were monitored through measurement of remaining surface area after 15 minutes, 30 minutes, 1 hour, 2 hours, 24 hours and 48 hours.

PCNA staining of relaxed collagen lattices

To determine proliferation, relaxed collagen lattices were fixed in HOPE solution (DCS, Hamburg, Germany), embedded in paraffin and sliced in 3 µm thin sections. Sections were stained with antibody against PCNA (see 2.1.3.). Signal detection was revealed using DCS Supervision detection kit (DCS, Hamburg, Germany). Slices were dehydrated through an increasing ethanol gradient (70% ethanol, 80% ethanol, 96% ethanol, 100% ethanol) cleared with xylene (Roth, Karlsruhe, Germany) and mounted with entelan (Merck,Darmstadt, Germany).

Pictures were taken using Olympus BX 40 (Olympus, Hamburg, Germany) and Cell D 3.4 Olympus Soft Imaging Solutions (Olympus, Hamburg, Germany).

2.2.2.4. Stressed collagen lattices

To force myofibroblast transdifferentiation primary lung fibroblasts (HEL299 or primary murine lung fibroblasts, see 2.2.2.1. and 2.2.2.2.) were embedded into stressed collagen lattices. Cells were trypsinized and counted with haemocytometer using trypan blue staining. Cells were seeded on ice in a concentration of 500 000 cells per lattice into stressed collagen gel mix consisting of 0.92 ml 1.76 x MEM , 0.12 ml Collagen I, Rat tail (Life Technologies, Darmstadt, Germany), 0.04 ml 0.1 M NaOH and 0.19 ml FBS (Biochrom AG, Berlin, Germany). Suspension was added to 3.5 cm Petri dishes (Sarstedt, Newton NC, USA) lined with 2.8 cm wide nylon rings. Lattices were incubated at 5 % CO_2 concentration and 37 °C. After eight hours stressed lattices were fixed with HOPE solution (DCS, Hamburg,

Germany) embedded in paraffin and sliced in 3 µm thin sections.

Anti smooth muscle actin staining of stressed collagen lattices

To detect myofibroblast transdifferentiation sections of relaxed and stressed collagen lattices as well as primary murine lung fibroblasts grown on coverslips for 12 days were stained with anti smooth-muscle actin Cy3 labeled antibody (see 2.1.3.). Counterstaining was performed with vimentin and DAPI (Life Technologies, Darmstadt, Germany). Sections were mounted aqueous using Dako Faramount mounting medium (Dako, Hamburg, Germany). Pictures were taken at 20 x and 40x magnification using Axiovert 200 and Axiovsion Imaging Software (Carl Zeiss, Jena, Germany).

2.2.3. Molecular biological methods

2.2.3.1. RNA extraction and quantitative real time PCR

Quantitative real-time PCR (qRT-PCR) was performed on whole cell lysates of lung fibroblasts (HEL299 or primary murine lung fibroblasts). Total RNA was isolated using Trizol reagent (Life Technologies, Darmstadt, Germany) and reverse transcription was performed using 1 µg total RNA and Super-Script III® VILO™-cDNA Synthesis Kit (Life Technologies, Darmstadt, Germany) according to the manufacturer´s protocol. Total cDNA was screened for CTGF, PAI-1, GAPDH, HPRT, B2M and LTBP4 using specific primers (2.1.4.). Quantitative changes in mRNA expression were assessed by qRT-PCR using Platinum® Quantitative PCR SuperMix-UDG w/ROX (Life technologies, Karlsruhe, Germany). Data were normalized by geometric averaging of three internal control genes (HPRT, GAPDH, B2M, see 2.1.4.) using geNorm

normalisation tool (geNorm plus, Biogazelle, Zwijnaarde, Belgium). Quantification of mRNA levels was calculated by using the ΔΔCt method.

2.2.4. Protein biochemical methods

2.2.4.1. Western Blot Analyses

Western blot analyses were performed on lung extracts from eight day old mice and whole cell lysates of primary human lung fibroblasts (see 2.2.2.1 and 2.2.2.2.). Lung Tissue and cell pellets were snap-frozen in liquid nitrogen, homogenized using mortar and resuspended in lysis buffer (10 mM HEPES, pH 7.9, 10 mM EDTA, 1 % Triton-X 100) containing protease inhibitor cocktail (Roche, Grenzach-Wyhlen, Germany). Total protein was quantified using the Lowry Protein Assay Kit (Bio-Rad Laboratories, Munich, Germany). 20 µg of total protein were resolved on 7.5% or 12% polyacrylamid gels and transferred to nitrocellulose membranes (Machery & Nagel, Düren, Germany) for immunoblotting. Blots were probed with primary antibodies (see 2.1.3.) while anti

GAPDH (see 2.1.3.) served as loading control. Densitometric analysis of bands was performed using ChemiDoc MP System imager (BioRad, Munich, Germany) and Image lab software (BioRad, Munich, Germany).

2.2.4.2. TGFβ activity assay

Reporter mink lung epithelial cells (MLECs) which produce luciferase in response to TGFβ1 where a kind gift of Prof. Daniel Rifkin (NYU Langone Medical Center, New York, USA). To test the amount of active and total TGFβ1 produced by primary murine lung fibroblasts, cells were incubated in MEM supplemented with 2% FBS (Biochrom AG, Berlin, Germany) and 1% Pen/Strep (Life Technologies, Darmstadt, Germany). After 48 hours supernatants were collected and the cell number was counted. The supernatant was splitted, one untreated part served as test samples to measure the concentration of active TGFβ1, one part was heat treated for 5 minutes at 80 °C degree, serving as a test sample to measure the concentration of total TGFβ1. Similarly, a

TGFβ1 standard curve (500pg, 250pg, 125pg, 62.5pg, 32.25pg, 15.6pg, 7.8pg, 3.9pg and 1.9pg using human recombinant TGFβ1 (R&D Systems, Minneapolis, MN, USA)) was prepared. MLECs were plated in 96-well plates (Sarstedt, Newton NC, USA) in a concentration of 1.6×10^4 cells per well and were allowed to attach for 3 hours in DMEM at 37°C in 5 % CO_2 supplemented with 200 µg/ml Geneticindisulfat. After 3 hours the supernatant was aspirated and test samples or standard curve were added to attached MLECs. Luciferase activity was measured using Beetle-Juice BIG kit (PJK, Kleinblittersdorf, Germany) in a Glomax Luminometer (Promega, Madison WI, USA).

2.2.5. Statistical analyses

Statistical analysis was performed on the results of histomorphometry, TGFβ activity assay, quantitative RT-PCR and western blot analysis. The results of quantitative RT-PCR were calculated based on the ΔΔCt method and expressed as fold induction of mRNA

expression compared to the corresponding control group. For quantitative protein analysis densitometry was performed and values were normalized to GAPDH. Statistical analysis was performed with GraphPad Prism (GraphPad Software Inc. San Diego, USA). Significance was determined by the nonparametric t-test (Mann-Whitney test). Error bars were calculated as SEM. Differences were considered to be statistically significant at values of $p<0.05$; P values are as indicated by asterisks: ***$p<0.001$, **$p<0.01$, *$p<0.05$.

3. Results

Ltbp4^{-/-} mice develop severe hypercapnia and polycytemia

Ltbp4^{-/-} mice die within the first ten days of life, after acute respiratory distress (Bultmann-Mellin et al. 2015). To decipher the aetiopathology before death, animals were sacrificed by decapitation at postnatal day eight and trunc blood analyses were performed. Compared to wildtype littermates, Ltbp4^{-/-} mice expressed a severe hypercapnia marked by a significant up-regulation of the partial pressure of carbon dioxide (pCO_2) and a polycytemia characterized by an increased level of haemoglobin (ctHb) and haematocrit (Hct) (figure 5.1).
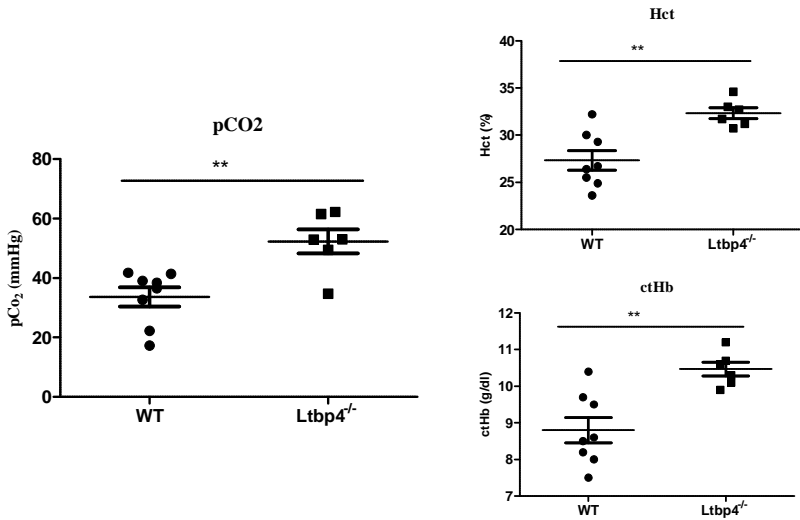
	Fold increase	P value	Mean ± SEM WT	Mean ± SEM Ltbp4 -/-	n
pCO$_2$	>1.5 fold	p=0.0035	33.66 ±3.232	52.30±4.087	6
ctHb	1.2 fold	p=0.0024	8.800±0.3454	10.47±0.1909	6
Hct	1.2 fold	p=0.0023	27.33±1.028	32.32±0.5793	6

Figure 3.1 Trunc blood analyses revealed severe hypercapnia and polycytemia in Ltbp4$^{-/-}$ mice

Trunc blood analyses of mice at P8. Ltbp4$^{-/-}$ mice depict a significant increase (over 1.5 fold) of the partial pressure of carbon dioxide (p=0.0035, n=6) and polycytemia marked by an elevated haemoglobin (ctHb) (1.2 fold; p=0.0024, n=6) and haematocrit (Hct) (1.2 fold; p=0.0023, n=6). Values are presented as means ± SEM.

Lack of Ltbp4 impairs postnatal alveolarisation in Ltbp4$^{-/-}$ mice

To investigate possible morphological alterations accounting for the clinical and laboratory findings, lung sections were histologically analysed. Hematoxylin and eosin (H&E) stainings as well as Ltbp4 immunostainings of lung tissue revealed a disrupted alveolarisation in Ltbp4$^{-/-}$ mice compared to wildtype littermates. At postnatal day eight, Ltbp4$^{-/-}$ mice displayed less septated alveoli, implicating an extreme enlargement of the alveolar space, compared to wildtype littermates. Parenchyma had a saccular morphology with an almost complete loss of septation (figure 3.2).
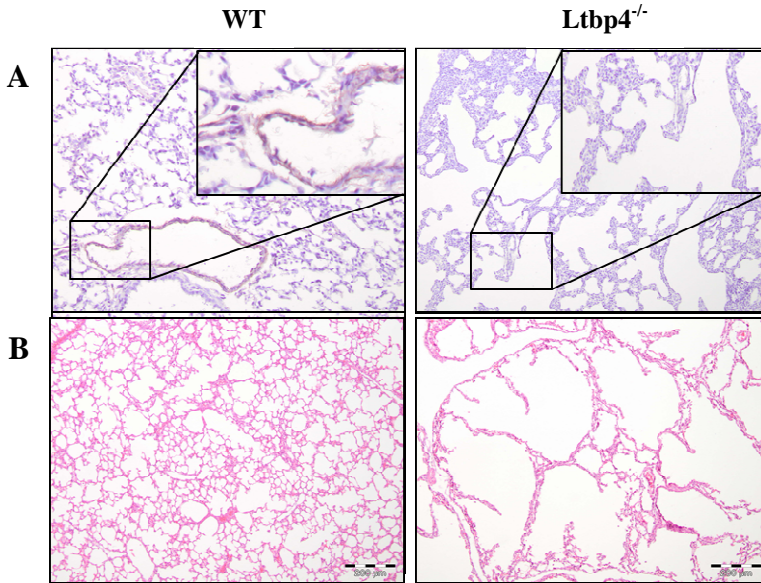
Figure 3.2 Lung tissue sections depict impaired postnatal alveolarisation in Ltbp4$^{-/-}$ mice

Representative Ltbp4 (A) and H&E (B) stained lung sections of P8 mice. Six animals per genotype were analysed, ten sections per animals were stained, five random fields were photographed (A) Ltbp4 staining depicts the distribution of Ltbp4 in lung tissue of wildtype mice (WT). Ltbp4 (red) is primarily located in the vascular endothelium and at the tips of alveoli. Ltbp4$^{-/-}$ mice (Ltbp4$^{-/-}$) express no Ltbp4 in the lung tissue (B). Physiological alveolarisation in wildtype mice (WT) compared to deficient alveolarisation in Ltbp4$^{-/-}$ mice (LTBP4$^{-/-}$).

To quantify the morphologic differences observed between Ltbp4$^{-/-}$ and wildtype lungs, morphometric analyses were performed, by measuring the mean linear intercept (MLI). The MLI describes the mean intra-alveolar distance and is approximately inversely proportional to the alveolar surface.
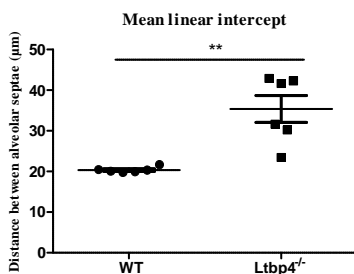
	Fold increase	P value	Mean ± SEM WT	Mean ± SEM Ltbp4$^{-/-}$	N
MLI	>1.5 fold	p=0.0011	20.37±0,2865	35.35±3.308	6

Figure 3.3 Mean linear intercept (MLI) depict impaired postnatal alveolarisation in Ltbp4$^{-/-}$ mice

Morphometric analyses of lung tissue sections of P8 old mice revealed a significant (p=0.0011) increase of the MLI in Ltbp4$^{-/-}$ mice compared to wildtype littermates (>1.5 fold, n=6). Values are presented as means ± SEM.

Morphometric analysis revealed a statistical significant increased MLI in lung tissue sections of Ltbp4^{-/-} mice in comparison to wildtype littermates (figure 3.3).

Impaired myofibroblast transdifferentiation in lung tissue of Ltbp4^{-/-} mice

To address whether the striking alterations in lung tissue morphology are associated with dysregulated key processes of postnatal alveolarisation, analyses on myofibroblast transdifferentiation and elastic fibre distribution were performed.

Myofibroblast transdifferentiation is a distinctive feature of postnatal alveolarisation. Transdifferentiated myofibroblasts are located at the entry ring of the newly formed alveolus and express αSMA (Schittny, Mund et al. 2008). To exhibit transdifferentiated myofibroblasts, lung tissue sections were stained against αSMA.

Tissue sections of eight day old Ltbp4$^{-/-}$ mice showed large areas of less αSMA positive myofibroblasts, compared to wildtype littermates (figure 3.4).
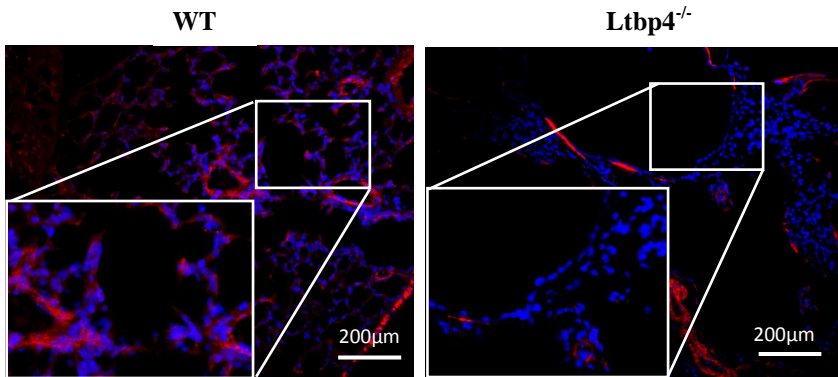
Figure 3.4 αSMA stained lung tissue sections depict impaired myofibroblast transdifferentiation in Ltbp4$^{-/-}$ mice

Representative slide of lung tissue sections. Lung tissue of Ltbp4$^{-/-}$ mice (Ltbp4$^{-/-}$) show large areas of less αSMA positive cells (red), compared to wildtype lung tissue (WT). (Cell nuclei – blue, αSMA- red).

There are two possible reasons for a reduced level of αSMA positive myofibroblasts in lung tissue, an increase of cellular degradation or a developmental failure.

To distinguish between degradation and disturbed transdifferentiation, *in vitro* experiments were performed. Fibroblasts grown in stressed collagen lattices under high tension or grown on cover slides over a longer period of time transdifferentiate into αSMA positive myofibroblasts (Tomasek, Haaksma et al. 1992).

Primary murine Ltbp4$^{-/-}$ lung fibroblasts (Ltbp4$^{-/-}$), grown over time to transdifferentiate on cover slides (figure 3.5 A) and in stressed collagen lattices (figure 3.5 B) show less myofibroblast transdifferentation compared to primary murine wildtype fibroblasts (WT). In addition αSMA positive fibres in Ltbp4$^{-/-}$ lung fibroblasts grown in stressed collagen lattices appeared patch like and unbranched compared to WT cells (figure 3.5 B).

WT **Ltbp4 $^{-/-}$**

A

B
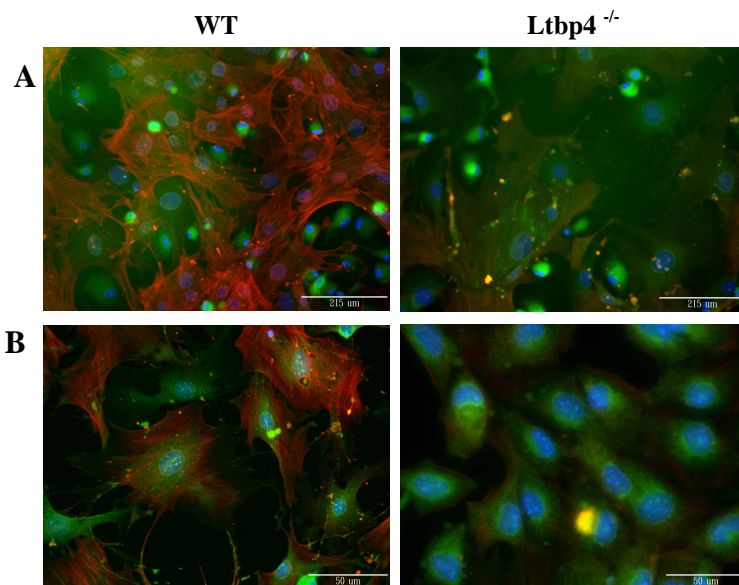
Figure 3.5 αSMA staining revealed impaired myofibroblast transdifferentiation in primary murine Ltbp4$^{-/-}$ lung fibroblasts

(A) Representative images of primary murine lung fibroblasts grown on glas cover slides for 12 days and stained against αSMA, Ltbp4$^{-/-}$ lung fibroblasts (Ltbp4$^{-/-}$) showed less αSMA positive cells (red), compared to wildtype fibroblasts (WT). (Cell nuclei – blue, vimentin – green, αSMA- red).

(B) Representative images of primary murine lung fibroblasts grown in stressed collagen lattices and stained against αSMA, Ltbp4$^{-/-}$ lung fibroblasts (Ltbp4$^{-/-}$) showed less αSMA positive cells (stained in red), compared to wildtype fibroblasts (WT). (Staining pattern: Cell nuclei – blue, vimentin – green, αSMA- red).

Disruption of elastic fibres in lung tissue of Ltbp4$^{-/-}$ mice

Alveolar elastin distribution and subsequent elastic fibre formation are inevitable for postnatal alveolarisation. To illustrate elastic fibre distribution and possible fibrotic ECM transformations, lung tissue sections are stained with Hart´s staining (Culling, Reid et al. 1974). Hart´s stained lung tissue sections of animals at postnatal day eight revealed aberrant alveolar elastic fibres in Ltbp4$^{-/-}$ mice (Ltbp4$^{-/-}$) compared to wildtype littermates (WT). Alveolar elastic fibres were fragmented and discontinuous in lung tissue of Ltbp4$^{-/-}$ mice (figure 3.6).
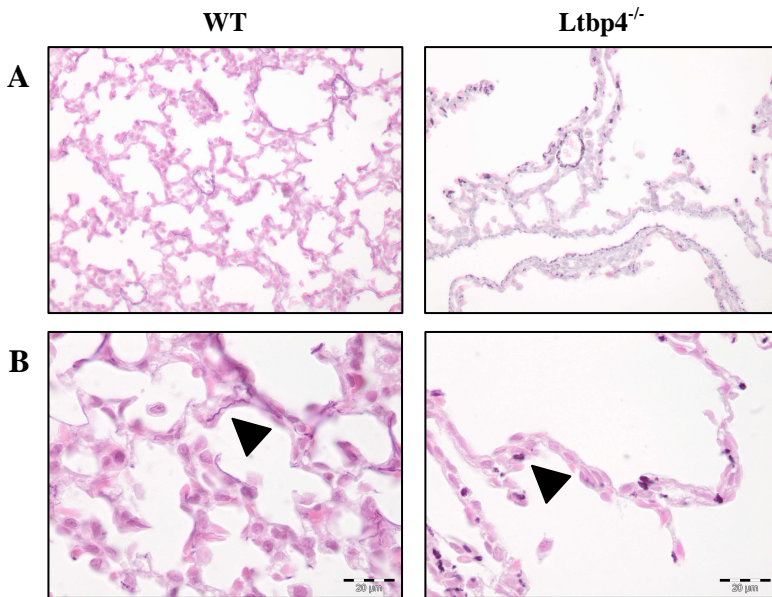
Figure 3.6 Hart´s staining of lung tissue sections revealed disruption of alveolar elastic fibres in Ltbp4$^{-/-}$ mice

Representative lung tissue sections of P8 old mice show patch like elastic fibres (arrowheads) in Ltbp4$^{-/-}$ mice (Ltbp4$^{-/-}$) compared to physiological elastic fibres in wildtype littermates (WT). Six animals per genotype were analysed, ten sections per animals were stained, five random fields were photographed Upper panel (A) 20x magnification, lower panel (B)

Characterisation of underlying molecular mechanisms of myofibroblast transdifferentiation in Ltbp4$^{-/-}$ mice

Impaired ability of matrix organisation of LTBP4$^{-/-}$ fibroblasts

Based on the fact that transmission of tractional forces from the extracellular matrix to the cells is necessary for myofibroblast transdifferentiation (Tomasek, Haaksma et al. 1992), the cell – matrix interaction of primary murine lung fibroblasts was tested. Due to matrix alignment and tractional forces fibroblasts grown in untethered collagen lattices contract. Therefore diameter reduction can be used as a scale unit for the ability of matrix organisation *in vivo*. Primary murine Ltbp4$^{-/-}$ lung fibroblasts and siRNA transfected human lung fibroblasts were grown in free floating untethered collagen lattices with low

stiffness. Lattice contraction was measured by diameter reduction.

Free floating untethered collagen lattices colonized with primary murine Ltbp4$^{-/-}$ lung fibroblasts (Ltbp4$^{-/-}$) for 48 hours revealed three fold less diameter reduction compared to free floating untethered collagen lattices colonized with wildtype fibroblasts (WT) (p<0.001, n=6).

Free floating untethered collagen lattices colonized with siRNA transfected, LTBP4 downregulated human lung fibroblasts (HEL 299) for 48 hours revealed four fold less diameter reduction compared to untransfected or mocktransfected human lung fibroblasts (p=0.0143, n=6) (figure 3.7).
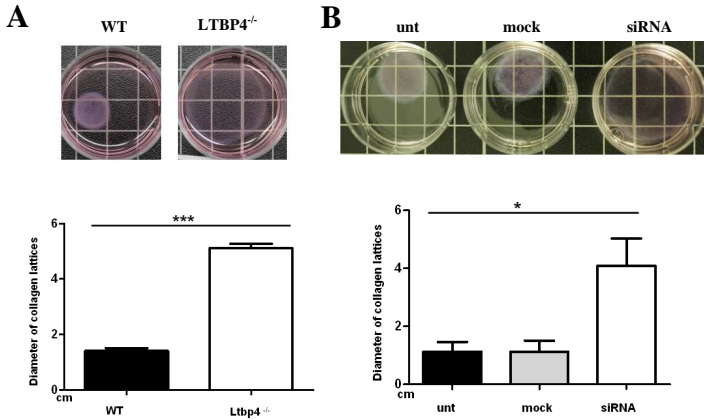
	Fold diameter reduction	P value	Mean ± SEM WT or mock transfected	Mean ± SEM LTBP4^{-/-}or siRNA transfected	n
Primary murine lung fibroblasts	3 fold	p<0.001	1.443 ±0.1058	5.109±0.1619	6
siRNA transfected human lung fibroblasts	4 fold	p=0.0143	1.128±0.3795	4.094±0.9442	6

Figure 3.7 Diameter reduction of untethered collagen lattices depict impaired ability of matrix structuration in LTBP4 deficient lung fibroblasts

Murine and human lung fibroblasts deficient of LTBP4 lack the ability of matrix structuration, marked by diameter reduction of three dimensional, free floating untethered collagen lattices.

(A) Primary murine lung fibroblasts isolated from Ltbp4$^{-/-}$mice (Ltbp4$^{-/-}$) exhibit significant (p<0.0001) less diameter reduction of free floating untethered collagen lattices compared to wildtype cells (WT), n=6.

(B) siRNA transfected, LTBP4 downregulated human embryonic lung fibroblasts (HEL 299) (siRNA) show less diameter reduction (p=0.0143) of free floating collagen lattices compared to untransfected (unt) and mocktransfected (mock) cells, n=6.

To validate the downregulation of LTBP4 in siRNA transfected human lung fibroblasts, qRT-PCR and western blot analyses were performed.

siRNA transfected human lung fibroblasts displayed a significant downregulation of LTBP4 120 hours post transfection. qRT- PCR analyses revealed a 40% reduction of LTBP4 on the mRNA level 120h post transfection compared to untransfected or mock transfected human lung fibroblasts (HEL 299) (figure 3.8 A).Western blot analyses show a 58% reduction of

LTBP4 post transfection compared to untransfected and mocktransfected human lung fibroblasts (HEL 299). Data presented as percentage band absorbance (figure 3.8 B).

A   **B**

	% reduction	P value	Mean ± SEM untransfected	Mean ± SEM siRNA transfected	n
HEL2 99	58%	p=0.0041	84.00±1.000	66.50±0.500	6
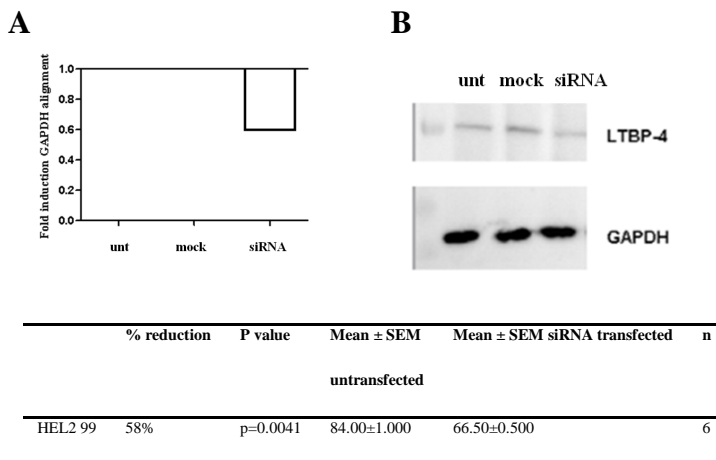
Figure 3.8 Downregulation of LTBP4 in siRNA transfected human lung fibroblasts(A) qRT-PCR analysis revealed a 40% reduction of LTBP4 in siRNA transfected human lung fibroblasts compared to untransfected and mocktransfected human lung fibroblasts (HEL 299) 120 hours post transfection.

(B) Western blot analysis revealed a 58% reduction of LTBP4 in siRNA transfected human lung fibroblasts compared to untransfected and mocktransfected human lung fibroblasts (HEL 299) 120 hours post transfection. Data presented as percentage band absorbance.

To address insufficient collagen lattice contraction to the impaired ability of matrix organisation and to exclude effects based on a reduced cellular viability, PCNA staining to visualise cell proliferation was performed on free floating untethered collagen lattices. Quantification of PCNA positive cells compared to the total number of cells revealed no significant difference between siRNA transfected LTBP4 downregulated human lung fibroblasts compared to untransfected human lung fibroblasts (slides of six untethered collagen lattices where stained, 100 cells where counted) (figure 3.9A and B).

A

B
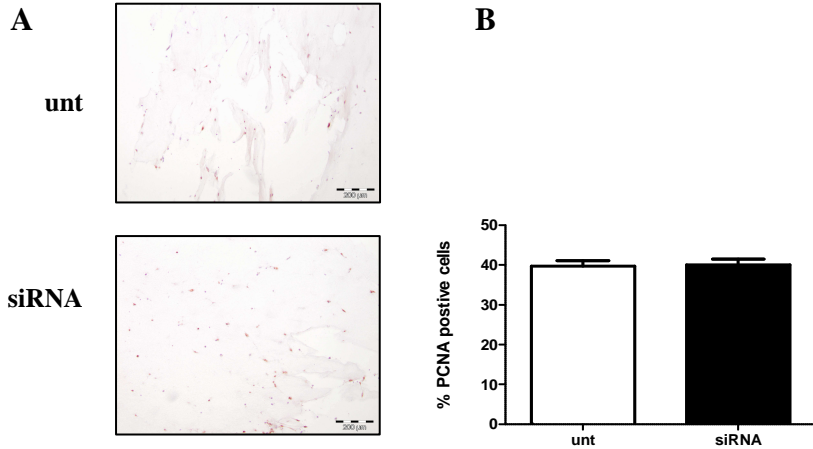
Figure 3.9 Proliferation of fibroblasts in free floating untethered collagen lattices

Proliferation of fibroblasts is not affected by lack of LTBP4

(A)   PCNA staining of human lung fibroblasts grown in free floating untethered collagen lattices illustrated no difference in PCNA staining (brown) of siRNA transfected LTBP4 downregulated human lung fibroblasts (siRNA) compared to untransfected human lung fibroblasts (unt).

(B)   Quantification of PCNA positive cells (brown) compared to PCNA negative cells (blue) revealed no significant difference in the proliferation rate of siRNA transfected LTBP4 downregulated human lung fibroblasts (siRNA) compared to untransfected human lung fibroblasts (unt). Readings in percentage PCNA positive cells to the total number of cells (100).

Ctgf and Pai-1 are negatively regulated in primary murine Ltbp4$^{-/-}$ lung fibroblasts

CTGF and PAI-1 are two genes that belong to the expression profile of transdifferentiated myofibroblasts (Kessler, Dethlefsen et al. 2001). To address whether alterations in the expression of αSMA positive myofibroblasts and the aberrant elastic fibres are associated with an altered expression of Ctgf and Pai-1, qRT-PCR analyses on primary murine Ltbp4$^{-/-}$ lung fibroblasts were performed.

Expression level of Ctgf and Pai-1 were decreased in primary murine Ltbp4$^{-/-}$ lung fibroblasts.

Ctgf expression was 96 % downregulated in primary murine Ltbp4$^{-/-}$ lung fibroblasts compared to primary murine wildtype lung fibroblasts (p=0.0004, B2M alignment).

94

Pai-1 expression was 95 % downregulated in primary murine Ltbp4$^{-/-}$ lung fibroblasts compared to primary murine wildtype lung fibroblasts. (p=0.0231, B2M alignment), (figure 3.10).
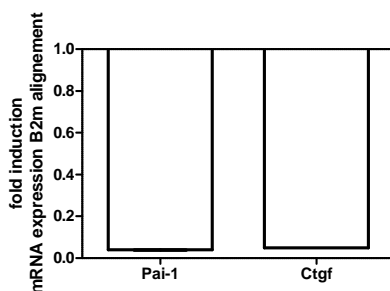
	% reduction	P value	Mean ± SEM WT fibroblasts	Mean ± SEM Ltbp4$^{-/-}$ fibroblasts	n
Ctgf	96 %	p=0.0004	1.000±0.02	0.0495±0.0005	3
Pai-1	95%	p=0. 0231	1.010±0.0.15	0.0395±0.0005	3

Figure 3.10 Expression of Ctgf and Pai-1 is downregulated in primary murine Ltbp4$^{-/-}$ lung fibroblasts.

qRT-PCR analysis of the expression pattern of Ctgf and Pai-1 revealed a downregulation in primary murine Ltbp4$^{-/-}$ lung fibroblasts. Ctgf expression was 96% downregulated and Pai-1 expression was 95% downregulated in primary murine Ltbp4$^{-/-}$ lung fibroblasts compared to wildtype fibroblasts (Ctgf p=0,0004, Pai-1 p=0,0231, n=3, B2M alignment).

To validate the results, qRT-PCR analyses on the expression level of CTGF and PAI-1 were performed on siRNA transfected LTBP4 silenced human lung fibroblasts. Expression level of CTGF was 20% (p=0.2505) and of Pai-1 (p=0.2821) was 15% decreased in siRNA transfected LTBP4 silenced human lung fibroblasts compared to untransfected human lung fibroblasts (B2M alignment) (figure 3.11)
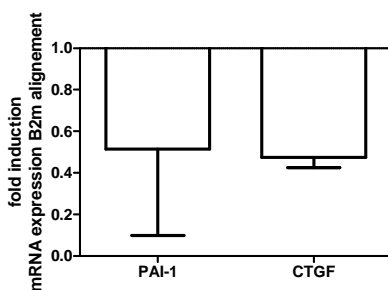
	% reduction	P value	Mean ± SEM mock	Mean ± SEM siRNA	N
CTGF	20 %	p=0.2505	1.435±0.475	0.0495±0.4750	3
PAI-1	15%	p=0. 2821	0.9200±0.6308	0.5150±0.4150	3

Figure 3.11 Expression of CTGF and PAI-1 is downregulated in LTBP4 silenced human lung fibroblasts (HEL 299).

qRT-PCR analysis of the expression pattern of CTGF and PAI-1 revealed a downregulation in siRNA transfected human lung fibroblasts (siRNA) compared to mocktransfected human lung fibroblasts (mock) (PAI-1: p=0,2821, Ctgf: p=0,2505, n=3, B2M alignment).

Tgfβ1 activity is altered in primary murine Ltbp4$^{-/-}$lung fibroblasts

CTGF and PAI-1 are also described as downstream targets of TGFβ1 (Grotendorst 1997, Kessler, Dethlefsen et al. 2001). Since LTBP4 is a chaperone of TGFβ1, the amount of active and total Tgfβ1 produced by primary murine lung fibroblasts were analysed.

The level of active Tgfβ1 was significantly increased in primary murine Ltbp4$^{-/-}$lung fibroblasts compared to wildtype fibroblasts (p=0.0491, figure 3.12 A). At the same time the level of total Tgfβ1 was decreased in primary murine Ltbp4$^{-/-}$lung fibroblasts compared to wildtype fibroblasts (p=0.0304, figure 3.12 B).
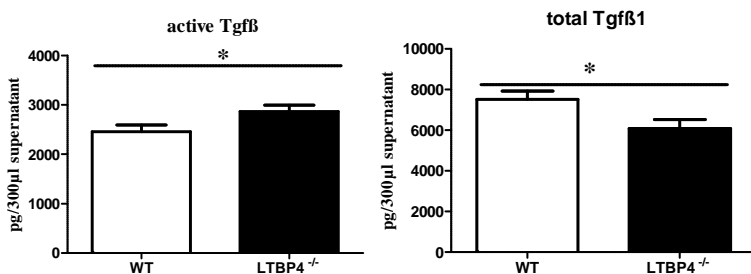
	P value	Mean ± SEM WT fibroblasts	Mean ± SEM Ltbp4$^{-/-}$fibroblasts	n
Total Tgfβ1	p=0.0491	2456±137.7	2864±133.2	9
Active Tgfβ1	p=0.0304	7520±410.2	6088±436.3	9

Figure 3.12 Tgfβ1 activity in primary murine lung fibroblasts

(A)Luciferase assay detecting the level of active Tgfβ1, produced by primary murine lung fibroblasts.

Supernatant of primary murine Ltbp4$^{-/-}$lung fibroblasts (Ltbp4$^{-/-}$) contained significant more active Tgfβ1 compared to wildtype lung fibroblasts (WT) (p=0.0491, n=9, data presented in pg/300µl supernatant).

(B) Luciferase assay, detecting total Tgfβ1, produced by primary murine lung fibroblasts.

Supernatant of primary murine Ltbp4$^{-/-}$lung fibroblasts (Ltbp4$^{-/-}$) contained significant less total Tgfβ1 compared to wildtype lung fibroblasts (WT) (p=0.0304, n=9, data presented in pg/300µl supernatant).

Downregulation of Ctgf and Pai-1 is reversible in primary murine Ltbp-4$^{-/-}$ lung fibroblasts

The expression of CTGF and PAI-1 is regulated in a complex manner. Two regulatory factors are described, mechano transduction (Kessler, Dethlefsen et al. 2001) and TGFβ1 (Grotendorst 1997). To analyse whether the downregulation of Ctgf and Pai-1 in primary murine Ltbp4$^{-/-}$ lung fibroblasts is reversible, fibroblasts are stimulated for 48 hours with 1ng and 2ng of human recombinant TGFβ1 and qRT-PCR analyses on the expression level of Ctgf and Pai-1 were performed.Expression levels of Pai-1 and Ctgf are significantly downregulated in unstimulated primary murine Ltbp4$^{-/-}$ lung fibroblasts compared to primary murine wildtype lung fibroblasts. 48 hours after stimulation with 1ng human recombinant TGFβ1 the

expression levels of Pai-1 and Ctgf in primary murine Ltbp4$^{-/-}$ lung fibroblasts are equal to the expression levels of Pai-1 and Ctgf in primary murine wildtype lung fibroblasts. Stimulation with 2ng human recombinant TGFβ1 leads to an overexpression of Pai-1 and Ctgf in primary murine Ltbp4$^{-/-}$ lung fibroblasts.

	P value	Mean ± SEM WT fibroblasts	Mean ± SEM Ltbp4^{-/-} fibroblasts unstimulated	n
Ctgf	p=0.0004	1.000±0.02	0.0495±0.0005	3
Pai-1	p=0.0231	1.010±0.15	0.0395±0.0005	3

	P value	Mean ± SEM WT fibroblasts	Mean ± SEM Ltbp4^{-/-}fibroblasts + 1ng TGFß1	n
Ctgf	p=0, 873	1.000±0.02	1.115±0.635	3
Pai-1	p=09447	1.010±0.1500	0.9650±0.5550	3
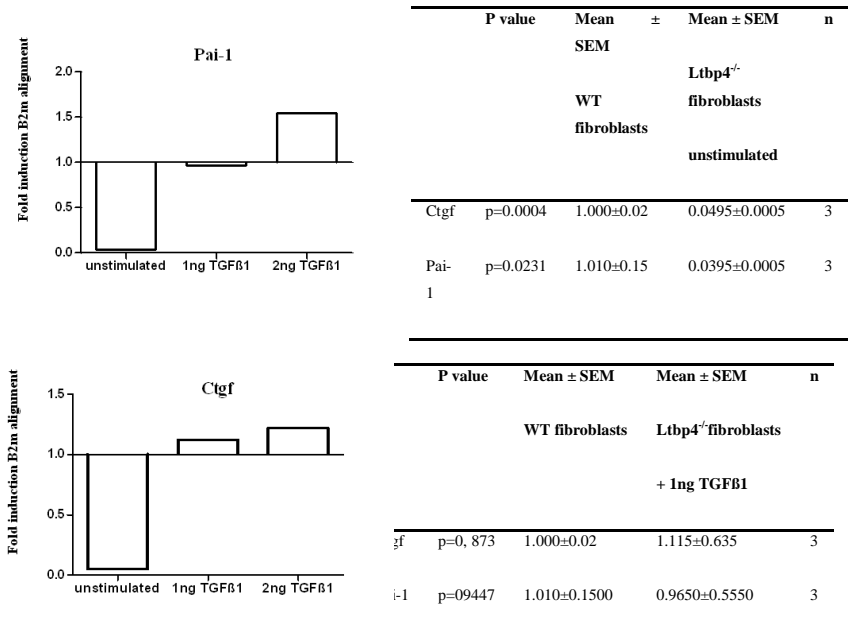
Figure 3.13 Downregulation of Ctgf and Pai-1 in primary murine Ltbp4^{-/-} lung fibroblasts is reversible

In primary murine Ltbp4^{-/-} lung fibroblasts (Ltbp4^{-/-}) a significant downregulation of Pai-1 and Ctgf compared to primary murine wildtype fibroblasts (WT) is evident (Data presented as fold induction, B2m alignment). Stimulation of primary murine Ltbp4^{-/-} lung fibroblasts results in a normalisation of the expression level of Pai-1(upper panel) and Ctgf (lower panel) to the expression level of primary murine wildtype fibroblasts. (Data presented as fold induction, B2m alignment)

101

4. Discussion

The latent TGFβ binding protein 4 (LTBP4) is a large extra cellular glycoprotein that shares structural homology with fibrillins (Todorovic and Rifkin 2012). Two functions of LTBP4 are reported so far: First it acts as a regulator of secretion, latency, storage and activation of TGFβ1 in the extracellular matrix (Todorovic, Jurukovski et al. 2005), second it is described as a distinct structural protein of the extracellular matrix (Kantola, Keski-Oja et al. 2008, Dabovic, Chen et al. 2009).

To date there are only few publications concerning the clinical manifestations associated with mutations in the *LTBP4* gene, amongst them Ltbp4 short form knockout mice published in 2002 (Sterner-Kock, Thorey et al. 2002) and human patients suffering from Urban Rifkin Davis syndrome (URDS) (Urban, Hucthagowder et al. 2009). Both mice and human patients develop diverse symptomes, such as cardiomyopathy, colorectal cancer in

mice and impaired gastrointestinal, genitourinary, musculoskeletal and dermal development in human patients. Despite a huge variety of highly tissue-specific abnormalities all individuals with disruptions of the *LTBP4* gene share one phenotype; alterations in pulmonary structure (Sterner-Kock, Thorey et al. 2002, Urban, Hucthagowder et al. 2009)

Disruption of LTBP4 leads to severe pulmonary emphysema culminating in lethal respiratory failure in humans and mice (Sterner-Kock, Thorey et al. 2002, Urban, Hucthagowder et al. 2009). Several studies have analysed LTBP4 in terms of matrix structuration (Kantola, Keski-Oja et al. 2008) and regulation of the bioavailability of TGFβ1 (Koli, Wempe et al. 2004) but none so far has focused on dysregulated processes during late lung development. Therefore this study aimed to elucidate the pathomechanisms of the development of pulmonary emphysema in Ltbp4$^{-/-}$mice. This is the first study analysing disrupted postnatal alveolarisation in a new Ltbp4$^{-/-}$ mouse model.

The purpose of the new complete knock out mouse model was to avoid any splicevariant specific effects. While humans express 3 LTBP4 splicevariants (LTBP¬4l1,LTBP¬4l2. LTBP¬4s) mice express 2 Ltbp4 splicevariants (Ltbp4l and Ltbp4s) Oklu and Hesketh 2000).

Our data demonstrate that the complete lack of Ltbp4 lead to severe hypercapnia in Ltbp4$^{-/-}$ mice at eight days post partum (see 3.1). As expected in accordance with this functional impairment, lung tissue of Ltbp4$^{-/-}$mice appears unseptated, with enlarged alveolar spaces. Alveoli are reduced in number and septal walls seem incomplete, a condition reminiscent to emphysema (see 3.2). Morphometric analysis through MLI measurement verifies a lack of alveolarisation in Ltbp4$^{-/-}$mice (see 3.3). These findings are in line with observations made in preceding studies analysing Ltbp4 short form knockout mice (Sterner-Kock, Thorey et al. 2002) and previous reports demonstrating abnormal lung development in human patients with disruptions of the *LTBP4* gene

suffering from URDS (Urban, Hucthagowder et al. 2009).

Ltbp4 short form knockout mice develop pulmonary emphysema. The emphysema aggravates with time so that by the age of six to eight month the lungs of Ltbp4 short form knockout mice exceeded the normal size by threefold. Histologically, alveolar spaces were enlarged, inflated, and significantly reduced in number (Sterner-Kock, Thorey et al. 2002). Human URDS patients have severe infantile bronchopulmonary dysplasia with developmental emphysema, cystic, and atelectatic abnormalities, hypoplastic lungs, and susceptibility to pneumonia (Urban, Hucthagowder et al. 2009). Considering the time course of lung development in humans and mice it is strikingly evident that in both Ltbp4$^{-/-}$ mice as well as in human URDS patients first clinical signs of respiratory failure become apparent at the same stage of late lung development, the stage of postnatal alveolarisation. Consequently this observation suggests a pivotal role of LTBP4 in late lung

development. In contrast to the early occurrence of the phenotype in Ltbp4$^{-/-}$mice and URDS patients, Ltbp4 short form knockout mice develop pulmonary emphysema after six to eight months (Sterner-Kock, Thorey et al. 2002). This delay implicates a compensatory effect of the long splice variant of LTBP4 in the development of pulmonary emphysema in Ltbp4 short form knockout mice. Despite the temporal analogy of the pathogenesis of pulmonary emphysema, Ltbp4$^{-/-}$ mice as well as human URDS patients, show a huge intra individual variety in the severity of pulmonary emphysema.

At the outset of postnatal alveolarisation, αSMA positive, transdifferentiated myofibroblasts migrate within nascent septae, depositing septal elastin (Schittny, Mund et al. 2008, Warburton, El-Hashash et al. 2010). This preformation of septae is essential for subsequent maturation processes, including interstitial thinning and vascularisation, aiming a functional respiratory membrane.

Myofibroblasts are highly specialised cells that combine the synthetic phenotype of fibroblasts with the cytoskeletal characteristics of contractile smooth muscle cells (Hinz, Phan et al. 2012). αSMA positive myofibroblasts are located at the alveolar entry ring and are supposed to perform both mechanical and synthetic duties (Warburton, El-Hashash et al. 2010). Platelet derived growth factor 2 alpha$^{-/-}$(Pdgf 2 alpha$^{-/-}$) mice fail to develop these alveolar myofibroblasts and disruption of alveologenesis becomes evident four days after birth. Distal air sacs become dilated and thin walled and by the age of ten days lungs of Pdgf 2 alpha$^{-/-}$mice appear grossly abnormal (Lindahl, Karlsson et al. 1997, Bostrom, Gritli-Linde et al. 2002). Haematoxylin & Eosin (H&E) stained tissue sections of Pdgf 2 alpha$^{-/-}$ mice at the age of ten days resemble H&E stained tissue sections of Ltbp4$^{-/-}$ mice of eight days (see 5.2(Lindahl, Karlsson et al. 1997, Bostrom, Gritli-Linde et al. 2002).). Lung tissue of Ltbp4$^{-/-}$ mice has a saccular morphology with an extreme enlargement of the alveolar space.

With regard to the phenotypic analogy of the lung tissue of myofibroblasts deficient Pdgf 2 alpha^{-/-} mice and Ltbp-4^{-/-} mice and based on the fact that myofibroblasts are the cells with the highest Ltbp4 expression level in murine lung tissue sections (Dabovic, Chen et al. 2010) the expression pattern of αSMA positive myofibroblasts in Ltbp4^{-/-} mice compared to wildtype littermates was determined. Interestingly immunohistochemical staining of lung tissue sections reveale decrease of αSMA positive myofibroblasts in Ltbp4^{-/-} mice (see 3.4). These data are contrary to findings in Ltbp4 short form knockout mice published in 2010 by Dabovic et al.. Ltbp4 short form knockout mice exhibit abnormalities in the distribution of myofibroblasts with an increase of αSMA-producing cells, assessed as an indicator of lung fibrosis (Araya and Nishimura 2010). Lung fibrosis is an interstitial lung disease attended by the formation of excess fibrous connective tissue, resulting in a loss of elasticity. Fibrotic diseases are commonly described as reparative or reactive processes. No signs of fibrosis where evident in

tissue sections of Ltbp4$^{-/-}$ mice. The development of lung fibrosis in Ltbp4 short form knockout mice is again implicating a compensatory effect of the long splice variant of Ltbp-4. The lack of fibrosis in Ltbp4$^{-/-}$ lung tissue in addition to the early occurrence of the described phenotype in Ltbp4$^{-/-}$ mice compared to Ltbp4 short form knockout mice implicates a more severe aetiopathology in Ltbp4$^{-/-}$ mice. On the strength of the severity and the early occurrence of the lethal lung pathology, lung tissue of Ltbp4$^{-/-}$ mice lacks the ability to develop reparative processes like fibrosis.

In addition to the *in vivo* studies the impact of LTBP4 on myofibroblast transdifferentiation was investigated *in vitro*. In agreement to our *in vivo* observations, less myofibroblast transdifferentation in primary murine Ltbp4$^{-/-}$ lung fibroblasts was observed (see 3.5). Moreover, we observed a reduced cell matrix interaction of primary murine Ltbp4$^{-/-}$ lung fibroblasts and siRNA transfected LTBP4 silenced human lung fibroblasts compared to primary murine wildtype fibroblasts and

untransfected human fibroblasts (see 3.7). Transfection experiments in rat lung fibroblasts have elucidated, that overexpression of αSMA in cultured fibroblasts enhances their contractile activity, thereby suggesting a correlation between αSMA expression and cell matrix interaction, represented by contractility (Hinz 2010). In summary, these data demonstrate that lack of LTBP4 leads to disruption of myofibroblast transdifferentiation in addition to reduction of cell contractility. Besides contractility, the second phenotypic property of myofibroblasts is the synthesis of ECM components, for example myofibroblasts are the major source of alveolar elastin (Tomasek, Gabbiani et al. 2002) .

Elastin is an important component of many organ systems that undergo repetitive physiological stress (Wendel, Taylor et al. 2000). In the lung alveolar elastin is located at the entry ring of each alveolus, conferring resilience and structural integrity, and thereby inevitable for the function of the mature organ. Alterations of elastic fibres lead to thinning and weakening of the

alveolar walls, followed by abnormal expansion of air sacs, and thereby resulting in pulmonary emphysema (Wendel, Taylor et al. 2000). In addition to its functional role in the adult lung, elastin is a critical morphogenetic force of alveologenesis (Noguchi, Reddy et al. 1989). Recent studies illustrate the correlation between disruption of alveolar elastin and abnormal lung development (Wendel, Taylor et al. 2000, Bostrom, Gritli-Linde et al. 2002). Mice lacking elastin ($Eln^{-/-}$) show defective postnatal lung development (Wendel, Taylor et al. 2000). Air sacs of $Eln^{-/-}$ lungs dilate at birth and secondary septation is attenuated. The severity of the phenotype increases by P2.5 and $Eln^{-/-}$ mice die at P3.5 in the saccular stage of postnatal lung development exhibiting severe pulmonary emphysema. In comparison mice failing myofibroblast transdifferentiation exhibit disrupted elastic fibre formation later in live at the stage of postnatal alveolarisation. Pdgf 2 $A^{-/-}$ mice develop sparse and discontinuous elastic fibres in the lung parenchyma, but elastic fibre morphology occurs normal

in blood vessels and bronchial walls (Bostrom, Gritli-Linde et al. 2002).

Previous studies of Ltbp4 short form knockout mice (Sterner-Kock, Thorey et al. 2002) and of human patients suffering from URDS (Urban, Hucthagowder et al. 2009) revealed major alterations of elastic fibres in the lung as well as in multiple other tissues. Consistent with these findings Ltbp4$^{-/-}$ mice exhibit severe alterations of the structure of elastic fibres in the lung (see 3.6), the blood vessels and other tissues ((Bultmann-Mellin, Conradi et al. 2015). Because of its incorporation into the ECM, its colocalisation with elastic fibres, and its structural resemblance to other fibrillins LTBP4 is supposed to be part of the microfibrillar core of elastic fibres (Kantola, Keski-Oja et al. 2008, Noda, Dabovic et al. 2013). Elastin interaction with microfibrils is essential for proper elastic fibre formation, called elastogenesis (Dabovic et al., 2011). In our study both, impaired myofibroblast transdifferentiation and disrupted elastic fibre formation result in severe alterations of postnatal

alveolarisation in Ltbp4$^{-/-}$ mice. Interestingly Tgfβ1 knockout mice show no alterations in elastic fibre formation and thereby don´t develop lung emphysema (McLennan, Poussart et al. 2000). These observations suggest a discrete function of LTBP4 in the ECM, independend of its role as a chaperone of TGFβ1.

Kessler et al. have identified a number of genes that belong to the expression profile of different activated fibroblasts amongst them αSMA positive myofibroblasts. Two of these genes are connective tissue growth factor (CTGF) and plasminogen activator inhibitor-1 (PAI-1) (Kessler, Dethlefsen et al. 2001). Both genes are thought to be regulated through mechano transduced tension. These considerations are in agreement with previous studies on wound healing, where tractional forces are inevitable for proper myofibroblast transdifferentiation (Tomasek, Haaksma et al. 1992, Phan 2008, Hinz, Phan et al. 2012). Ltbp4 deficiency decreases expression of Ctgf and Pai-1 in primary murine Ltbp4$^{-/-}$ lung fibroblasts and siRNA transfected LTBP4 downregulated human

lung fibroblasts (HEL 299) (see 5.11). In addition to tension-induction of gene expression, CTGF and PAI-1 are downstream targets of TGFβ1 through autocrine and paracrine mechanisms (Grotendorst 1997, Iwaki, Urano et al. 2012). The influence of disruption of LTBP4 on the TGFβ1 signalling is controversly discussed throughout the different publications:

Sterner-Kock et al. revealed on the basis of immunohistochemical analysis on lung tissue sections of Ltbp4 short form knockout mice a complete lack of extracellular Tgfβ1 (Sterner-Kock, Thorey et al. 2002). In addition to these findings Dabovic et al. described an increased level of active Tgfβ1 in Ltbp4 short form knockout lungs (Dabovic, Chen et al. 2009). Investigations on fibroblasts of human URDS patients have shown a significant increase of active TGFβ1, while mRNA levels of TGFβ1 were normal (Urban, Hucthagowder et al. 2009). Considering the fact that TGFβ1 is stored and kept latent in the ECM by LTBP4 a simultaneous decrease of ECM linked latent TGFβ1 with

an increase of active TGFβ1 after disruption of LTBP4 is allegeable. In line with previous studies the level of active Tgfβ1 secreted by primary murine Ltbp4$^{-/-}$ lung fibroblasts was increased compared to wildtype fibroblasts (see 3.12 A). At the same time the level of total Tgfβ1 was decreased in primary murine Ltbp4$^{-/-}$lung fibroblasts compared to murine wildtype fibroblasts (see 3.12 B). Interestingly the expression of Ctgf and Pai-1 are not affected by the increase of active Tgfβ1 in primary murine Ltbp4$^{-/-}$ lung fibroblasts. In contrast Ctgf and Pai-1 expression is reduced in primary murine Ltbp4$^{-/-}$ lung fibroblasts (see 3.10).

Time course expression analysis of CTGF expression in fibroblasts grown in attached collagen lattices have shown, that CTGF expression is independent to high TGFβ1 and induction appears to be directly by mechanical tension (Kessler, Dethlefsen et al. 2001). This is in contrast to previous reports, suggesting that TGFβ1 regulates CTGF expression (Grotendorst 1997, Iwaki, Urano et al. 2012). Interestingly our results

decipher, that supplementation of 1ng human recombinant TGFβ1 to primary murine Ltbp4$^{-/-}$lung fibroblasts rescued the expression of Ctgf and Pai-1 (see 3.13), thereby suggesting that the regulation of CTGF and PAI-1 is dependent of both, mechanical tension and TGFβ1.

Taken together, this study confirmed that LTBP4 has a strong impact on postnatal alveolarisation. Two key processes of postnatal alveolarisation: Myofibroblast transdifferentiation and alveolar elastic fibre formation are disrupted in Ltbp4$^{-/-}$ mice. LTBP4 therefore plays a pivotal role in myofibroblast transdifferentiation as well as elastogenesis during late lung development.

5. Zusammenfassung

Strukturelle und Funktionelle Analyse von LTBP 4 als Faktor der Pathogenese des Lungenemphsems

Im Jahr 2009 veröffentlichte die Arbeitsgruppe um Davis erstmals vier Fälle von humanen Patienten welche ein komplexes Krankheitsbild zeigten, das Urban-Rifkin-Davis Syndrom (URDS) (Urban, Hucthagowder et al. 2009). Alle beschriebenen Fälle hatten Mutationen im Latent Transforming growth factor β (TGFβ) bindenden Protein 4 (LTBP4). LTBP4 ist eines von vier Latent TGFβ bindenden Proteinen (LTBP1-4). Namensgebend für die Familie der LTBP Moleküle ist die enge Interaktion mit (TGFβ). Neben der Beteiligung von LTBP4 im TGFβ1 Signalweg gibt es jedoch Hinweise, dass LTBP4 zusätzlich eine Funktion als Strukturprotein der extrazellulären Matrix (ECM) erfüllt.

Mutationen des *LTBP4* Genes resultieren in einer Vielzahl von Erkrankungen. Vorangegangene Studien haben gezeigt, dass Knockoutmäuse denen die kurze Variante des Ltbp4 (Ltbp4s) fehlt ein komplexes Krankheitsbild mit unter anderem Störungen des Herz-Kreislaufsystems und des Atmungstraktes ausbilden. URDS Patienten zeigen Veränderungen im Gastrointestinaltrakt, Urogenitaltrakt, der Haut und der Lunge. Allen Individuen mit Mutationen im *LTBP4* Gen ist dabei die Entwicklung von Lungenemphysemen im Stadium der postnatalen Alveolarisation gemeinsam.

Um durch Splicevarianten verursachte Effekte auszuschließen, wurden in dieser Studie erstmals bis dato noch nicht beschriebene Ltbp4 komplett Knockout - Mäuse (Ltbp4$^{-/-}$ Mäuse) untersucht.

Ziel war die Analyse der Rolle von LTBP4 als Faktor in der Pathogenese von Lungenemphysemen.

Ltbp4$^{-/-}$ Mäuse wurden mittels Blutgasanalysen und Lungenhistologischen Untersuchungen charakterisiert.

118

Sowohl primäre murine Ltbp4$^{-/-}$ Lungenfibroblasten, als auch siRNA transfizierte LTBP4 defiziente humane Lungenfibroblasten wurden im Hinblick auf Myofibroblastentransdifferenzierung, Matrixstrukturierung und TGFβ Aktivität untersucht.

Ltbp4$^{-/-}$ Mäuse versterben innerhalb der ersten zehn Lebenstage nach schwerer Hyperkapnie und Polyzytämie. Das Lungengewebe zeigt eine verminderte Alveolarisation, fragmentierte elastische Fasern in den Alveolen und reduzierte myofibroblasten Transdifferenzierung.

In vitro zeigten die LTBP4 defizienten humanen und murinen Lungenfibroblasten eine gestörte Strukturierung der extrazellulären Matrix.

Zusammengefasst sind sowohl die Myofibroblastendifferenzierung als auch weitere Schlüsselmechanismen der postnatalen Alveolarisation, wie die Bildung von alveolären elastischen Fasern bei Ltbp4$^{-/-}$ Mäusen gestört. Diese Studie ist die erste, die

eine gestörte postnatale Alveolarisation im Zusammenhang mit Mutationen im *LTBP4* Gen untersucht und gibt neue Einblicke in die Funktion von LTBP-4 als Faktor in der Lungenentwicklung.

6. Summary

The American Journal of Human Genetics published in 2009 four cases of newborn children with a complex disease pattern, the Urban-Rifkin-Davis Syndrome (URDS). All patients had mutations of the *Latent TGFβ binding Protein 4 (LTBP4)* gene. LTBP4 is one of four known LTB proteins. Eponymous for this protein family is the strong interaction with Transforming growth factor β (TGFβ). In addition LTBP4 it is assumed as a distinct structural protein of the ECM.

Disruption of LTBP4 leads to a variety of disease patterns. Preceding studies have shown that mice lacking the short variant of Ltbp4 (Ltbp4s) develop a complex phenotype with cardiomyopathy, colorectal cancer and pulmonary emphysema. Human patients suffering URDS exhibit impaired pulmonary, gastrointestinal, genitourinary, musculoskeletal and dermal development. Despite a huge variety of disease patterns all individuals with mutations in the *LTBP4* gene share one phenotype;

the development of pulmonary emphysema at the stage of postnatal alveolarisation.

Aim of this study was the structural and functional analysis of LTBP4 as a factor of pathogenesis in the development of pulmonary emphysema.

To avoid any splicevariant specific effects, Ltbp4 complete knockout mice (Ltbp4$^{-/-}$) were analysed via assessment of oxygenation and lung structure. *In vitro* investigations on myofibroblast transdifferentation, matrix structuration and TGFβ activation were performed on primary murine Ltbp4$^{-/-}$ lung fibroblasts as well as siRNA transfected, LTBP4 deficient human lung fibroblasts.

Ltbp4$^{-/-}$ mice die within the first ten days of life with severe hypercapnia and polycythemia. Lung tissue of Ltbp4$^{-/-}$ mice exhibit impaired alveolarisation, disrupted alveolar elastic fibre distribution and reduced myofibroblast transdifferentation. Both primary Ltbp4$^{-/-}$ lung fibroblasts as well as siRNA transfected, LTBP4

deficient human lung fibroblasts revealed impaired matrix structuration *in vitro.*

In summary two key processes of postnatal alveolarisation: myofibroblast transdifferentation and alveolar elastic fibre formation are disrupted in Ltbp4$^{-/-}$ mice, thereby implicating the pivotal role of LTBP4 during alveolarisation. This is the first study investigating the impact of Ltbp4 on postnatal alveolarisation by means of a new animal model, the Ltbp4$^{-/-}$ model.

7. References

Alejandre-Alcazar, M. A., M. Michiels-Corsten, A. G. Vicencio, I. Reiss, J. Ryu, R. R. de Krijger, G. G. Haddad, D. Tibboel, W. Seeger, O. Eickelberg and R. E. Morty (2008). "TGF-beta signaling is dynamically regulated during the alveolarization of rodent and human lungs." <u>Dev Dyn</u> **237**(1): 259-269.

Araya, J. and S. L. Nishimura (2010). "Fibrogenic reactions in lung disease." <u>Annu Rev Pathol</u> **5**: 77-98.

Bartram, U., D. G. Molin, L. J. Wisse, A. Mohamad, L. P. Sanford, T. Doetschman, C. P. Speer, R. E. Poelmann and A. C. Gittenberger-de Groot (2001). "Double-outlet right ventricle and overriding tricuspid valve reflect disturbances of looping, myocardialization, endocardial cushion differentiation, and apoptosis in TGF-beta(2)-knockout mice." <u>Circulation</u> **103**(22): 2745-2752.

Beyer, T. A., M. Narimatsu, A. Weiss, L. David and J. L. Wrana (2012). "The TGFbeta superfamily in stem cell biology and early mammalian embryonic development." <u>Biochim Biophys Acta</u>.

Bostrom, H., A. Gritli-Linde and C. Betsholtz (2002). "PDGF-A/PDGF alpha-receptor signaling is required for lung growth and the formation of alveoli but not for early lung branching morphogenesis." <u>Dev Dyn</u> **223**(1): 155-162.

Bourbon, J., O. Boucherat, B. Chailley-Heu and C. Delacourt (2005). "Control mechanisms of lung alveolar development and their disorders in bronchopulmonary dysplasia." <u>Pediatr Res</u> **57**(5 Pt 2): 38R-46R.

Bragg, A. D., H. L. Moses and R. Serra (2001). "Signaling to the epithelium is not sufficient to mediate all of the effects of transforming growth factor beta and bone morphogenetic protein 4 on murine embryonic lung development." <u>Mech Dev</u> **109**(1): 13-26.

Brown, R. A., R. Prajapati, D. A. McGrouther, I. V. Yannas and M. Eastwood (1998). "Tensional homeostasis in dermal fibroblasts: mechanical responses to mechanical loading in three-dimensional substrates." <u>J Cell Physiol</u> **175**(3): 323-332.

Bultmann-Mellin, I., A. Conradi, A. C. Maul, K. Dinger, F. Wempe, A. P. Wohl, T. Imhof, F. T. Wunderlich, A. C. Bunck, T. Nakamura, K. Koli, W. Bloch, A. Ghanem, A. Heinz, H. von Melchner, G. Sengle and A. Sterner-Kock (2015). "Modeling autosomal recessive cutis laxa type 1C in mice reveals distinct functions for Ltbp-4 isoforms." <u>Dis Model Mech</u> **8**(4): 403-415.

Burri, P. H. (2006). "Structural aspects of postnatal lung development - alveolar formation and growth." <u>Biol Neonate</u> **89**(4): 313-322.

Callewaert, B., C. T. Su, T. Van Damme, P. Vlummens, F. Malfait, O. Vanakker, B. Schulz, M. Mac Neal, E. C. Davis, J. G. Lee, A. Salhi, S. Unger, K. Heimdal, S. De Almeida, U. Kornak, H. Gaspar, J. L. Bresson, K. Prescott, M. E. Gosendi, S. Mansour, G. E. Pierard, S.

Madan-Khetarpal, F. C. Sciurba, S. Symoens, P. J. Coucke, L. Van Maldergem, Z. Urban and A. De Paepe (2012). "Comprehensive clinical and molecular analysis of 12 families with type 1 recessive cutis laxa." <u>Hum Mutat</u>.

Chandramouli, A., J. Simundza, A. Pinderhughes and P. Cowin (2011). "Choreographing metastasis to the tune of LTBP." <u>J Mammary Gland Biol Neoplasia</u> **16**(2): 67-80.

Chen, H., J. Sun, S. Buckley, C. Chen, D. Warburton, X. F. Wang and W. Shi (2005). "Abnormal mouse lung alveolarization caused by Smad3 deficiency is a developmental antecedent of centrilobular emphysema." <u>Am J Physiol Lung Cell Mol Physiol</u> **288**(4): L683-691.

Chen, S., M. Rong, A. Platteau, D. Hehre, H. Smith, P. Ruiz, J. Whitsett, E. Bancalari and S. Wu (2011). "CTGF disrupts alveolarization and induces pulmonary hypertension in neonatal mice: implication in the pathogenesis of severe bronchopulmonary dysplasia." <u>Am J Physiol Lung Cell Mol Physiol</u> **300**(3): L330-340.

Chen, Y. G., A. Hata, R. S. Lo, D. Wotton, Y. Shi, N. Pavletich and J. Massague (1998). "Determinants of specificity in TGF-beta signal transduction." <u>Genes Dev</u> **12**(14): 2144-2152.

Colarossi, C., Y. Chen, H. Obata, V. Jurukovski, L. Fontana, B. Dabovic and D. B. Rifkin (2005). "Lung alveolar septation defects in Ltbp-3-null mice." <u>Am J Pathol</u> **167**(2): 419-428.

Copland, I. and M. Post (2004). "Lung development and fetal lung growth." <u>Paediatr Respir Rev</u> **5 Suppl A**: S259-264.

Culling, C. F., P. E. Reid, M. G. Clay and W. L. Dunn (1974). "The histochemical demonstration of O-acylated sialic acid in gastrointestinal mucins. Their association with the potassium hydroxide-periodic acid-schiff effect." <u>J Histochem Cytochem</u> **22**(8): 826-831.

Dabovic, B., Y. Chen, J. Choi, E. C. Davis, L. Y. Sakai, V. Todorovic, M. Vassallo, L. Zilberberg, A. Singh and D. B. Rifkin (2010). "Control of lung development by latent TGF-ss binding proteins." <u>J Cell Physiol</u>.

Dabovic, B., Y. Chen, J. Choi, M. Vassallo, H. C. Dietz, F. Ramirez, H. von Melchner, E. C. Davis and D. B. Rifkin (2009). "Dual functions for LTBP in lung development: LTBP-4 independently modulates elastogenesis and TGF-beta activity." <u>J Cell Physiol</u> **219**(1): 14-22.

Dugina, V., L. Fontao, C. Chaponnier, J. Vasiliev and G. Gabbiani (2001). "Focal adhesion features during myofibroblastic differentiation are controlled by intracellular and extracellular factors." <u>J Cell Sci</u> **114**(Pt 18): 3285-3296.

Eitzman, D. T., R. D. McCoy, X. Zheng, W. P. Fay, T. Shen, D. Ginsburg and R. H. Simon (1996). "Bleomycin-induced pulmonary fibrosis in transgenic mice that either lack or overexpress the murine plasminogen activator inhibitor-1 gene." <u>J Clin Invest</u> **97**(1): 232-237.

Gauldie, J., T. Galt, P. Bonniaud, C. Robbins, M. Kelly and D. Warburton (2003). "Transfer of the active form of transforming growth factor-beta 1 gene to newborn rat lung induces changes consistent with bronchopulmonary dysplasia." <u>Am J Pathol</u> **163**(6): 2575-2584.

Grinnell, F. (2000). "Fibroblast-collagen-matrix contraction: growth-factor signalling and mechanical loading." Trends Cell Biol **10**(9): 362-365.

Grotendorst, G. R. (1997). "Connective tissue growth factor: a mediator of TGF-beta action on fibroblasts." Cytokine Growth Factor Rev **8**(3): 171-179.

Grotendorst, G. R., G. R. Martin, D. Pencev, J. Sodek and A. K. Harvey (1985). "Stimulation of granulation tissue formation by platelet-derived growth factor in normal and diabetic rats." J Clin Invest **76**(6): 2323-2329.

Heng, M. C. (2011). "Wound healing in adult skin: aiming for perfect regeneration." Int J Dermatol **50**(9): 1058-1066.

Hinz, B. (2010). "The myofibroblast: paradigm for a mechanically active cell." J Biomech **43**(1): 146-155.

Hinz, B., G. Celetta, J. J. Tomasek, G. Gabbiani and C. Chaponnier (2001). "Alpha-smooth muscle actin expression upregulates fibroblast contractile activity." Mol Biol Cell **12**(9): 2730-2741.

Hinz, B., S. H. Phan, V. J. Thannickal, M. Prunotto, A. Desmouliere, J. Varga, O. De Wever, M. Mareel and G. Gabbiani (2012). "Recent developments in myofibroblast biology: paradigms for connective tissue remodeling." Am J Pathol **180**(4): 1340-1355.

Hokuto, I., A. K. Perl and J. A. Whitsett (2003). "Prenatal, but not postnatal, inhibition of fibroblast growth factor receptor signaling causes emphysema." J Biol Chem **278**(1): 415-421.

Iwaki, T., T. Urano and K. Umemura (2012). "PAI-1, progress in understanding the clinical problem and its aetiology." Br J Haematol **157**(3): 291-298.

Jankov, R. P. and A. Keith Tanswell (2004). "Growth factors, postnatal lung growth and bronchopulmonary dysplasia." Paediatr Respir Rev **5 Suppl A**: S265-275.

Kaartinen, V., J. W. Voncken, C. Shuler, D. Warburton, D. Bu, N. Heisterkamp and J. Groffen (1995). "Abnormal lung development and cleft palate in mice lacking TGF-beta 3 indicates defects of epithelial-mesenchymal interaction." Nat Genet **11**(4): 415-421.

Kajekar, R. (2007). "Environmental factors and developmental outcomes in the lung." Pharmacol Ther **114**(2): 129-145.

Kantola, A. K., J. Keski-Oja and K. Koli (2008). "Fibronectin and heparin binding domains of latent TGF-beta binding protein (LTBP)-4 mediate matrix targeting and cell adhesion." Exp Cell Res **314**(13): 2488-2500.

Kantola, A. K., M. J. Ryynanen, F. Lhota, J. Keski-Oja and K. Koli (2010). "Independent regulation of short and long forms of latent TGF-beta binding protein (LTBP)-4 in cultured fibroblasts and human tissues." J Cell Physiol **223**(3): 727-736.

Kapanci, Y., C. Ribaux, C. Chaponnier and G. Gabbiani (1992). "Cytoskeletal features of alveolar myofibroblasts and pericytes in normal human and rat lung." J Histochem Cytochem **40**(12): 1955-1963.

Kessler, D., S. Dethlefsen, I. Haase, M. Plomann, F. Hirche, T. Krieg and B. Eckes (2001). "Fibroblasts in mechanically stressed collagen lattices assume a "synthetic" phenotype." J Biol Chem **276**(39): 36575-36585.

Koli, K., F. Wempe, A. Sterner-Kock, A. Kantola, M. Komor, W. K. Hofmann, H. von Melchner and J. Keski-Oja (2004). "Disruption of LTBP-4 function reduces TGF-beta activation and enhances BMP-4 signaling in the lung." J Cell Biol **167**(1): 123-133.

Kondaiah, P., M. Taira, U. D. Vempati and I. B. Dawid (2000). "Transforming growth factor-beta5 expression during early development of Xenopus laevis." Mech Dev **95**(1-2): 207-209.

Koski, C., J. Saharinen and J. Keski-Oja (1999). "Independent promoters regulate the expression of two amino terminally distinct forms of latent transforming growth factor-beta binding protein-1 (LTBP-1) in a cell type-specific manner." J Biol Chem **274**(46): 32619-32630.

Lindahl, P., L. Karlsson, M. Hellstrom, S. Gebre-Medhin, K. Willetts, J. K. Heath and C. Betsholtz (1997). "Alveogenesis failure in PDGF-A-deficient mice is coupled to lack of distal spreading of alveolar smooth muscle cell progenitors during lung development." Development **124**(20): 3943-3953.

Martin, P. (1997). "Wound healing--aiming for perfect skin regeneration." Science **276**(5309): 75-81.

Massague, J. (1998). "TGF-beta signal transduction." Annu Rev Biochem **67**: 753-791.

McGowan, S. E., R. E. Grossmann, P. W. Kimani and A. J. Holmes (2008). "Platelet-derived growth factor receptor-alpha-expressing cells localize to the alveolar entry ring and have characteristics of myofibroblasts during pulmonary alveolar septal formation." Anat Rec (Hoboken) **291**(12): 1649-1661.

McLennan, I. S., Y. Poussart and K. Koishi (2000). "Development of skeletal muscles in transforming growth factor-beta 1 (TGF-beta1) null-mutant mice." Dev Dyn **217**(3): 250-256.

Millan, F. A., F. Denhez, P. Kondaiah and R. J. Akhurst (1991). "Embryonic gene expression patterns of TGF beta 1, beta 2 and beta 3 suggest different developmental functions in vivo." Development **111**(1): 131-143.

Min, H., D. M. Danilenko, S. A. Scully, B. Bolon, B. D. Ring, J. E. Tarpley, M. DeRose and W. S. Simonet (1998). "Fgf-10 is required for both limb and lung development and exhibits striking functional similarity to Drosophila branchless." Genes Dev **12**(20): 3156-3161.

Noda, K., B. Dabovic, K. Takagi, T. Inoue, M. Horiguchi, M. Hirai, Y. Fujikawa, T. O. Akama, K. Kusumoto, L. Zilberberg, L. Y. Sakai, K. Koli, M. Naitoh, H. von Melchner, S. Suzuki, D. B. Rifkin and T. Nakamura (2013). "Latent TGF-beta binding protein 4 promotes elastic fiber assembly by interacting with fibulin-5." Proc Natl Acad Sci U S A **110**(8): 2852-2857.

Noguchi, A., R. Reddy, J. D. Kursar, W. C. Parks and R. P. Mecham (1989). "Smooth muscle isoactin and elastin in fetal bovine lung." Exp Lung Res **15**(4): 537-552.

Oklu, R. and R. Hesketh (2000). "The latent transforming growth factor beta binding protein (LTBP) family." Biochem J **352 Pt 3**: 601-610.

Pan, H. and J. Halper (2003). "Cloning, expression, and characterization of chicken transforming growth factor beta 4." Biochem Biophys Res Commun **303**(1): 24-30.

Pelton, R. W., M. D. Johnson, E. A. Perkett, L. I. Gold and H. L. Moses (1991). "Expression of transforming growth factor-beta 1, -beta 2, and -beta 3 mRNA and protein in the murine lung." Am J Respir Cell Mol Biol **5**(6): 522-530.

Pelton, R. W. and H. L. Moses (1990). "The beta-type transforming growth factor. Mediators of cell regulation in the lung." Am Rev Respir Dis **142**(6 Pt 2): S31-35.

Phan, S. H. (2008). "Biology of fibroblasts and myofibroblasts." Proc Am Thorac Soc **5**(3): 334-337.

Rock, J. R. and B. L. Hogan (2011). "Epithelial progenitor cells in lung development, maintenance, repair, and disease." Annu Rev Cell Dev Biol **27**: 493-512.

Roth-Kleiner, M. and M. Post (2003). "Genetic control of lung development." Biol Neonate **84**(1): 83-88.

Saharinen, J., M. Hyytiainen, J. Taipale and J. Keski-Oja (1999). "Latent transforming growth factor-beta binding proteins (LTBPs)--structural extracellular matrix proteins for targeting TGF-beta action." Cytokine Growth Factor Rev **10**(2): 99-117.

Schittny, J. C., S. I. Mund and M. Stampanoni (2008). "Evidence and structural mechanism for late lung alveolarization." Am J Physiol Lung Cell Mol Physiol **294**(2): L246-254.

Schmid, P., D. Cox, G. Bilbe, R. Maier and G. K. McMaster (1991). "Differential expression of TGF beta 1, beta 2 and beta 3 genes during mouse embryogenesis." Development **111**(1): 117-130.

Shi, W., N. Heisterkamp, J. Groffen, J. Zhao, D. Warburton and V. Kaartinen (1999). "TGF-beta3-null mutation does not abrogate fetal lung maturation in vivo by glucocorticoids." Am J Physiol **277**(6 Pt 1): L1205-1213.

Shipley, J. M., R. P. Mecham, E. Maus, J. Bonadio, J. Rosenbloom, R. T. McCarthy, M. L. Baumann, C. Frankfater, F. Segade and S. D. Shapiro (2000). "Developmental expression of latent transforming growth factor beta binding protein 2 and its requirement early in mouse development." Mol Cell Biol **20**(13): 4879-4887.

Singer, II, D. W. Kawka, D. M. Kazazis and R. A. Clark (1984). "In vivo co-distribution of fibronectin and actin fibers in granulation tissue: immunofluorescence and electron microscope studies of the fibronexus at the myofibroblast surface." J Cell Biol **98**(6): 2091-2106.

Skalli, O., P. Ropraz, A. Trzeciak, G. Benzonana, D. Gillessen and G. Gabbiani (1986). "A monoclonal antibody against alpha-smooth muscle actin: a new probe for smooth muscle differentiation." J Cell Biol **103**(6 Pt 2): 2787-2796.

Sorokin, S. P. (1970). "Properties of alveolar cells and tissues that strengthen alveolar defenses." <u>Arch Intern Med</u> **126**(3): 450-463.

Sterner-Kock, A., I. S. Thorey, K. Koli, F. Wempe, J. Otte, T. Bangsow, K. Kuhlmeier, T. Kirchner, S. Jin, J. Keski-Oja and H. von Melchner (2002). "Disruption of the gene encoding the latent transforming growth factor-beta binding protein 4 (LTBP-4) causes abnormal lung development, cardiomyopathy, and colorectal cancer." <u>Genes Dev</u> **16**(17): 2264-2273.

Todorovic, V., V. Jurukovski, Y. Chen, L. Fontana, B. Dabovic and D. B. Rifkin (2005). "Latent TGF-beta binding proteins." <u>Int J Biochem Cell Biol</u> **37**(1): 38-41.

Todorovic, V. and D. B. Rifkin (2012). "LTBPs, more than just an escort service." <u>J Cell Biochem</u> **113**(2): 410-418.

Tomasek, J. J., G. Gabbiani, B. Hinz, C. Chaponnier and R. A. Brown (2002). "Myofibroblasts and mechano-regulation of connective tissue remodelling." <u>Nat Rev Mol Cell Biol</u> **3**(5): 349-363.

Tomasek, J. J., C. J. Haaksma, R. J. Eddy and M. B. Vaughan (1992). "Fibroblast contraction occurs on release of tension in attached collagen lattices: dependency on an organized actin cytoskeleton and serum." <u>Anat Rec</u> **232**(3): 359-368.

Urban, Z., V. Hucthagowder, N. Schurmann, V. Todorovic, L. Zilberberg, J. Choi, C. Sens, C. W. Brown, R. D. Clark, K. E. Holland, M. Marble, L. Y. Sakai, B. Dabovic, D. B. Rifkin and E. C. Davis (2009). "Mutations in LTBP4 cause a syndrome of impaired pulmonary, gastrointestinal, genitourinary, musculoskeletal, and dermal development." Am J Hum Genet **85**(5): 593-605.

Vicencio, A. G., C. G. Lee, S. J. Cho, O. Eickelberg, Y. Chuu, G. G. Haddad and J. A. Elias (2004). "Conditional overexpression of bioactive transforming growth factor-beta1 in neonatal mouse lung: a new model for bronchopulmonary dysplasia?" Am J Respir Cell Mol Biol **31**(6): 650-656.

Warburton, D., A. El-Hashash, G. Carraro, C. Tiozzo, F. Sala, O. Rogers, S. De Langhe, P. J. Kemp, D. Riccardi, J. Torday, S. Bellusci, W. Shi, S. R. Lubkin and E. Jesudason (2010). "Lung organogenesis." Curr Top Dev Biol **90**: 73-158.

Warburton, D., M. Schwarz, D. Tefft, G. Flores-Delgado, K. D. Anderson and W. V. Cardoso (2000). "The molecular basis of lung morphogenesis." Mech Dev **92**(1): 55-81.

Wendel, D. P., D. G. Taylor, K. H. Albertine, M. T. Keating and D. Y. Li (2000). "Impaired distal airway development in mice lacking elastin." Am J Respir Cell Mol Biol **23**(3): 320-326.

Yoshinaga, K., H. Obata, V. Jurukovski, R. Mazzieri, Y. Chen, L. Zilberberg, D. Huso, J. Melamed, P. Prijatelj, V. Todorovic, B. Dabovic and D. B. Rifkin (2008). "Perturbation of transforming growth factor (TGF)-beta1 association with latent TGF-beta binding protein yields inflammation and tumors." Proc Natl Acad Sci U S A **105**(48): 18758-18763.

8. Acknowledgements

Herzlich möchte ich mich bei Frau Prof. Dr. Sterner Kock für die Bereitstellung des Themas und Ihre herzliche und fachkompetente Unterstützung in den letzten drei Jahren bedanken.

Herrn Professor Dr. Schmidt möchte ich herzlich für die Unterstützung in den vergangenen Jahren und die Möglichkeit an meiner Alma mater zu promovieren danken.

Frau Dr. Anne Conradi danke ich für die Betreuung der Arbeit und die geduldige Unterstützung.

Der Jürgen-Manchot Stiftung möchte ich für Ihre hervorragende Unterstützung danken.

Ganz besonders bedanken möchte ich mich

Bei Frau Ingrid Greiwe für die freundschaftliche und fachkompetente Hilfe bei der Bewältigung der

alltäglichen bürokratischen Hürden und in allen Lebenslagen.

Bei Frau Petra Heid für die kompetente Unterstützung bei der Bändigung der primären Zellkultur.

Bei Frau Andrea Elbers der Fachkraft für Primer und Aliquots.

Bei Frau Reinhild Brinker für ihre kompetente Unterstützung bei Western Blots und anderen Mysterien.

Bei Frau Manuela Lerwe für Kuchen und Freundschaft.

Bei Frau Irmgard Henke für Tipps bei allem was leuchtet oder auch nicht.

Bei Frau Bernadette Hartmann für ihren liebevollen Umgang mit Zwei- und Vierbeinern.

Bei Herrn Dr. Florian Hofmaier für seine immer ehrliche und freundschaftliche Beratung. Es war immer wieder gut auch mal eine männliche Sicht der Dinge zu sehen!

Bei Frau Ramona Braun für Ihre Freundschaft. Durch dich sind viele Stunden leichter geworden! Es war mir eine Ehre deinen Schleier zu tragen.

Bei Frau Dr. Marion Kramlich, für die vielen Gespräche, die guten Cocktails, die Sorgentelefonate, das Oktoberfest und vieles mehr.

Bei dem Team der Kinder- und Jugendmedizin für ihre freundschaftliche Unterstützung.

Ihr Alle habt es durch Eure Hilfe und Unterstützung geschafft, dass ich die letzten drei Jahre mit Freude zu meiner Arbeit gegangen bin. Danke!

Herrn Dr. Dr. Miguel Alejandre Alcazar danke ich für seinen Glauben an mich. Ohne Dich hätte ich an vielen Stellen aufgegeben.

Meinem Vater und meiner Mutter danke ich für Ihre Liebe und bedingungslose Unterstützung.

Meinem Bruder Sebastian, dass er mich gelehrt hat Ellenbogen zu zeigen.

Meiner großen Liebe meinem Mann Björn danke ich, dass es ihn gibt! Durch Deine Liebe und Zuversicht, weiß ich was wichtig ist.

9. Erklärung

Hiermit bestätige ich, dass ich die vorliegende Arbeit selbstständig angefertigt habe. Ich versichere, dass ich ausschließlich die angegebenen Quellen und Hilfen in Anspruch genommen habe.

Köln, den